Combination of Thermal and Seismic Displacements for the Design of Base Isolation Systems of Bridges in Canada

By

Philippe Brisebois

Department of Civil Engineering and Applied Mechanics
McGill University
Montreal, Canada
March, 2012

A thesis submitted to the
Faculty of Graduate Studies and Research
in partial fulfillment of the requirements for the degree of
Master of Science

Combination of Thermal and Seismic Displacements for the Design of Base Isolation Systems of Bridges in Canada

Abstract

Base isolation systems are commonly used in the design of new bridges, and in the retrofit of existing ones. However, in Canada, base isolators are relatively new. They act as bridge bearings and isolate or decouple the superstructure from the underlying substructure to reduce the force generated in the structure by ground-motions. Horizontal displacements of isolators due to thermal and seismic loads are addressed in the Canadian Highway Bridge Design Code (CHBDC) CSA-S6-06 and adequate clearance must be provided. However, the Canadian code does not offer any guidance on how to combine these displacements. The objective of this thesis is to present the calculation methods of these displacements and to suggest different ways to combine them. Two bridges are analyzed in this thesis under Montreal's and Vancouver's thermal and seismic provisions to define a proposed thermal and seismic displacement combination formula for the design of base isolators in bridges in Canada.

Résumé

Les isolateurs sismiques sont utilisés de plus en plus couramment pour la conception des nouveaux ponts ou pour la réfection des ponts existants. Or, ces isolateurs sont relativement nouveaux au Canada. En général, ils protègent la structure du pont en découplant le mouvement du sol du mouvement de la structure et en augmentant la période de vibration afin de réduire les accélérations transmises à la structure. Ces appuis sont conçus pour des déplacements admissibles spécifiés. La norme canadienne des ponts (CSA-S6) adresse les déplacements sismiques et thermiques, mais n'offre aucune directive sur la combinaison de ces déplacements. L'objectif de ma thèse est de présenter les méthodes de calcul pour ces déplacements et de suggérer diverses approches pour faire la combinaison des déplacements. Les ponts de Madrid et de l'autoroute 30 au-dessus du fleuve St-Laurent sont analysés sous les charges sismiques et thermiques de Montréal et Vancouver pour établir une combinaison optimale des déplacements sismiques et thermiques des isolateurs sismiques des ponts au Canada.

Acknowledgements

I would like to express my most sincere appreciation and gratitude to my advisor, Professor Luc E. Chouinard, for his guidance, support and advice during my Master's studies. Not only did his knowledge and experience greatly contribute to my understanding, but it also played a major role in my academic pursuit and fulfillment.

I would also like to thank the entire McGill Civil Engineering Department for providing all the necessary tools I needed to complete this journey. As well, I would like to acknowledge the financial support by the NSERC CREATE program and ACFAS, which aided the completion of this thesis.

Finally, I would like to acknowledge the assistance of Professor Gail M. Atkinson and Professor Katsuichiro Goda throughout this process and my family for their support and love.

Table of Contents

List of Figures

List of Tables

List of Abbreviations

AASHTO	American Association of State Highway and Transportation Officials
AB06	Atkinson and Boore's 2006 Earthquake Ground-Motion Relations for Eastern North America
AG10	Atkinson and Goda's 2010 Interim Updated Seismic Hazard Model
CHBDC	Canadian Highway Bridge Design Code
CSA	Canadian Standards Association
EDC	Energy Dissipation per Cycle
EPS	Earthquake Protection Systems
FPI	Friction Pendulum Isolation
GMPE	Ground Motion Prediction Equation
GSC	Geological Survey of Canada
HITEC	Highway Innovative Technology Evaluation Center
LRB	Lead Core Rubber Bearing
LRFD	Load Resistance Factor Design
NBCC	National Building Code of Canada
NEBT	New England Bulb Tee
NEHRP	National Earthquake Hazards Reduction Program
NZTA	New Zealand Transport Agency
PGA	Peak Ground Acceleration
PGV	Peak Ground Velocity
PTFE	Polytetrafluoroethylene
PSHA	Probabilistic Seismic Hazard Analysis
UHS	Uniform Hazard Spectrum

Chapter 1 Introduction and Literature Review

Bridges are considered critical infrastructures and are essential to the sound operation of a city in today's fast paced world. Every day, people use them for different reasons, but with one goal in mind: to save time. In order to do so, their traffic demand must be efficiently managed, while providing a high level of safety at a reasonable cost. Seismic design requirements in the Canadian Highway Bridge Design Code (CHBDC) evolve continuously and have increased significantly over the years. Major earthquakes, such as the 1995 Kobe and 2002 Central Alaska earthquakes, highlighted deficiencies in bridge seismic design standards and contributed to their improvement. In Canada, two seismic regions impose high risks to bridges. They are Canada's west coast due to the "Ring of Fire" circling the Pacific Ocean, and the east coast along the valley of the St-Lawrence River and Ottawa River. The government, conscious of their threats, is currently investing large sums of money to improve our infrastructures, and new cost-effective solutions are continuously being developed to protect bridges in strong earthquake zones.

This chapter reviews the evolution of seismic design provisions of the CHBDC, and in particular the design implications for seismic base isolation systems. It concludes with a description of the main base isolation systems used in Canada.

1.1 Seismic Design Evolution

Recently, significant technological improvements and refinements have been made to help engineers design earthquake resistant bridges. Seismic design requirements were first introduced in the CHBDC in 1966. Since then, many changes have been made. For instance, in the 1966 code, only the equivalent static force method of analysis was recommended for seismic design of bridges. Additionally, the 1966 code did not provide seismic loadings for different Canadian regions (CSA, 1966). By the 1978 edition of the code, the equivalent seismic static force Q, which was based on the seismic performance zone of the bridge, was prescribed for regular bridges. However, the code mentioned that Q also depended on the elastic seismic response coefficient C of the California response spectra database, and was deemed a conservative and safe approach for Canada at the time. Another important feature of the 1978 edition was that dynamic analyses were, for the first time, considered necessary for structures having a natural period of vibration larger than 3.0 seconds or for bridges located in unusual geological site conditions (CSA, 1978). Ten years later, the same two methods of analyses were still proposed, but refined by introducing new factors such as a risk factor I equal to 1.3 for important bridges and 1.0 for other bridges. Finally, the 1988 CHBDC referred engineers to the Supplement to the 1985 National Building Code of Canada (NBCC) for zone specific seismic loads (CSA, 1988).

In the latest two editions of the CHBDC, 2000 and 2006, engineers now have access to a whole chapter dedicated to seismic design of bridges (Chapter 4). The equivalent static force method, known as the ‘uniform-load’ method, is still

recommended, but only for regular emergency-route bridges and other bridges in low or moderate seismic performance zones. Dynamic methods are mostly used for all other scenarios and are known as single-mode spectral or multi-mode spectral methods. The time-history analysis is the last method recommended and is suggested for irregular lifeline bridges in high seismic performance zones. Coefficients are still used in the different analyses, but they have evolved over the years. For example, the importance factor I varies from 3.0 for lifeline bridges to 1.0 for other bridges, and the seismic zoning coefficients are now provided in the code through the zonal acceleration ratio A. Currently, not only do engineers have more elaborate and rational analysis methods, but, over the past few decades, the Geological Survey of Canada (GSC) has increased significantly its seismic database. As a result, the seismic loads in the 2000 and 2006 editions of the code increased considerably and are more realistic. Unfortunately, when compared to the NBCC, the latest two editions of the CHBDC haven't improved nearly as much as they should have. The CSA-S6-06 still ignores the fact that earthquakes are different in nature in the eastern and western seismic regions of Canada. What is more, nowhere in the code does it suggest to use the newly developed seismic hazard maps and uniform hazard spectra (UHS) developed by the Geological Survey of Canada (GSC) (CSA, 2000; CSA, 2006a).

Finally, engineers are currently rethinking ways to improve the seismic design approach, leaning towards a displacement-based design instead of a force-based design. This change is believed necessary since it has been proven that a bridge's ability to survive earthquakes is more a matter of its displacement capacity than its initial yield strength (Priestley & Kowalsky, 2000). Also, since 2000, a clause was created in the

CHBDC for seismic base isolation systems (Clause 4.10). These innovative systems have proven to be a viable economical option over the full life-cycle of a structure and can be used in bridge retrofitting as well as new construction in high seismic regions.

1.2 Seismic Design Philosophy

The philosophy adopted in the latest version of the CHBDC displacement based capacity design is the same as the 2004 version of the American Association of State Highway and Transportation Officials (AASHTO) load resistance factor design (LRFD) to achieve the desired performance criteria for bridges (CSA, 2006a; AASHTO, 2004). The seismic design section of the Canadian Code, states that all bridges must remain open to traffic immediately after a small to moderate earthquake, and must avoid collapse after a large earthquake (1000-year return period). That being said, the seismic performance requirements of a bridge depend on its importance category. The basis of classification of bridges takes into consideration socio-economic and security requirements. Table 1.1 summarizes the seismic performance requirements of bridges in Canada, according to their importance category.

Table 1.1: Seismic performance requirements of bridges in Canada (CSA, 2006a)

Return Period	**Bridge**		
	Lifeline	**Emergency-route**	**Other**
Small to moderate earthquake	All traffic Immediate use	All traffic Immediate use	All traffic Immediate use
Design earthquake (475-year return period)	All traffic Immediate use	Emergency vehicles Immediate use	Repairable damage
Large earthquake (1000 year-return period)	Emergency vehicles Immediate use	Repairable damage	No collapse

Conventional seismic design of bridges utilizes capacity design to dissipate the energy resulting from ground shaking. Careful detailing of the ductile substructure section of the bridge is highly important since inertia forces, during earthquakes, impose considerable stresses to the elements of the bridge connected to the ground surface. In addition, the substructure supports the greater part of the mass of the bridge; making it even more critical. This method prevents the need to design for maximum elastic seismic forces, since yielding is assumed to occur in the sub-structural elements of the bridge. Capacity design ensures that the substructure performs as the main energy dissipater while the other components of the bridge respond elastically. Inelastic hinging in the substructure is designed to occur above ground surface, since underground inspections and repairs are difficult and expensive. In the code, the elastic seismic load is reduced by the response modification factor R. This accounts for the ductility and redundancy of the structure. Therefore, the infrastructure is designed for a much lower seismic demand compared to the elastic seismic loading of the site. However, since the 2000 edition of the CHBDC, an alternative safe and economical seismic design method is proposed and requires isolator units.

1.3 Seismic Base Isolation Design

Seismic base isolation design, first employed at the turn of the 20th century, is certainly not a new idea. The first few bridges using seismic base isolators were designed in the 1970's. In Canada, they were not utilized until the 1990's. According to Priestley et

al. (1996), the three alternative methods to conventional ductile seismic design method are:

1) Passive systems
2) Active systems
3) Hybrid systems

Passive systems use base isolators combined with supplemental mechanical energy-dissipating devices with self-centring capabilities. The focus of this thesis is on passive systems and is described in more depth hereunder. Active systems rely solely on active mechanical devices to react to the response of the structure. Hybrid systems combine passive and active systems such that the structure's safety is not compromised even if the active system fails.

Ultimately, seismic base isolation decouples the superstructure of the bridge from its underlying substructure in order to reduce the damaging effects of ground accelerations. One of its main goals is to increase the structure's fundamental period of vibration away from the dominant frequencies of the earthquake ground-motion and the fundamental frequency of the fixed base superstructure. However, an increase in displacement demand is expected and needs to be accommodated within the flexible mount. Another important goal of seismic isolation is to provide sufficient extra damping into the system by mechanical energy-dissipating devices to limit the transmitted acceleration into the superstructure to a practical design level. Lastly, the flexible bridge must be rigid under frequently occurring low (service) load levels such as wind and braking forces to maintain its structural integrity (CSA, 2006b).

Base isolation systems or passive systems are usually located at the base of a structure. For bridges, however, since substructure elements are relatively lighter than superstructure members, base isolators are positioned on top of piers and abutments, acting as bridge bearings. Figure 1.1 illustrates a typical location for base isolators in bridges.

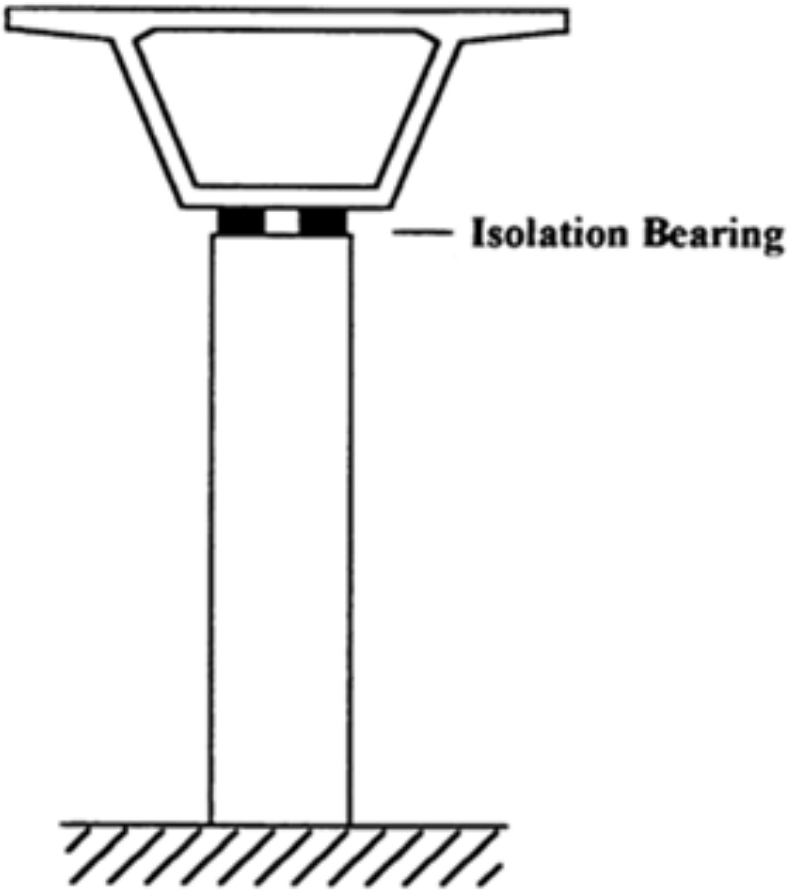

Figure 1.1: Location of base isolators in bridges (Chen & Duan, 2000)

A typical elastic response spectra is shown in Figure 1.2 representing the effect of increased period of vibration and damping with passive systems for bridges.

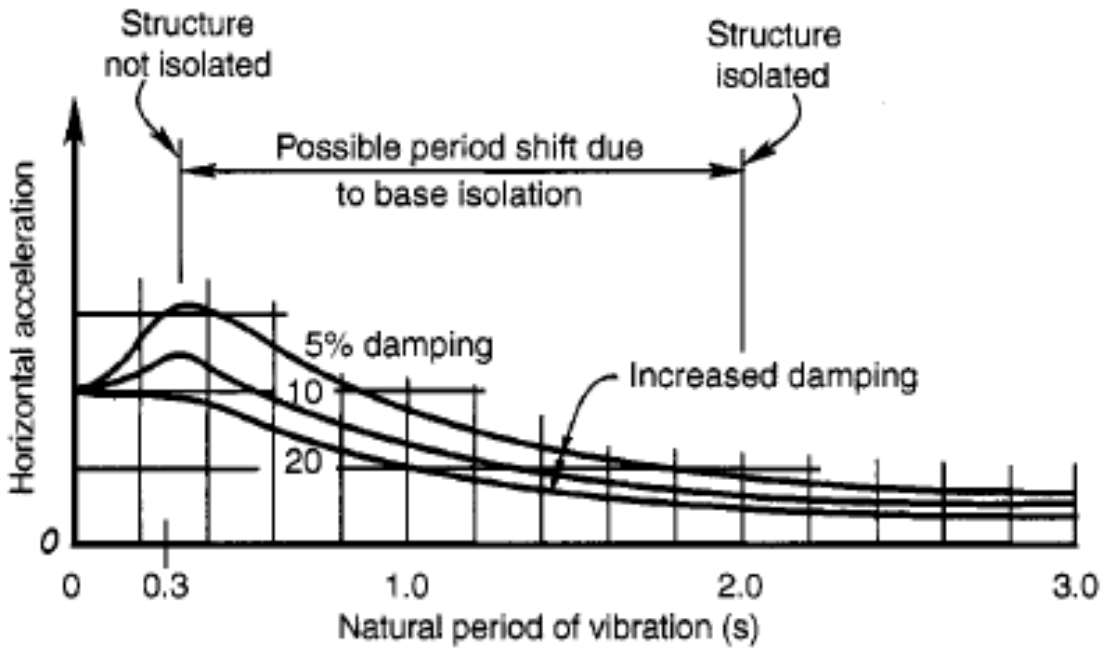

Figure 1.2: Typical design elastic response spectra for different damping systems (Milne, Ritchie, & Karihaloo, 2003)

When the bridge's natural period of vibration is increased, the horizontal acceleration is reduced significantly. For example, when the natural period of vibration increases from 0.3 s to approximately 2.0 s, the horizontal acceleration is reduced by roughly 70%. Furthermore, if damping is increased, acceleration is expected to be reduced even more. Conversely, Figure 1.3 depicts that when the period of vibration is lengthened, the displacement demand of the base isolators will increase. To minimize this demand during ground shaking, extra damping is needed. Consequently, engineers must design base isolation systems in order to find a compromise between reducing forces transferred from substructure to superstructure and limit displacements due to lengthening the period of vibration.

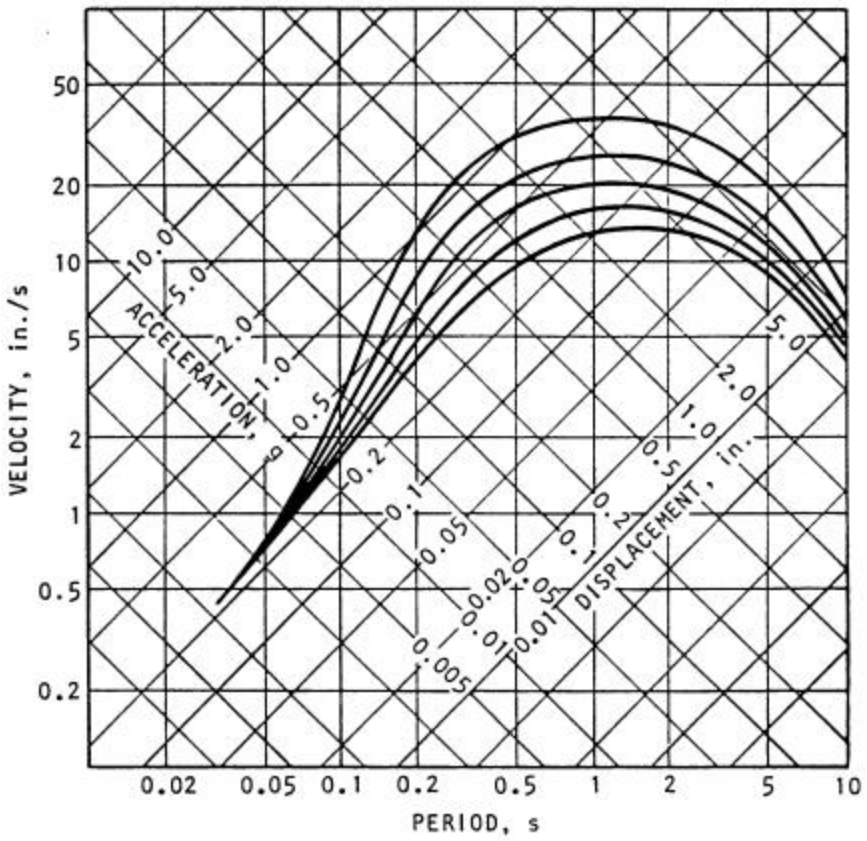

Figure 1.3: Typical smoothed design spectrum (Chen & Duan, 2000)

Nonlinear dynamic analysis is generally recommended by the Code for base isolation design of structures, since the isolators are inelastic in nature. Therefore, isolation systems need self-centring capabilities, since residual displacements may occur after ground shaking. Bridges with short to intermediate natural periods of vibration will generally benefit from a flexible mounting system. However, the site conditions of each bridge must be carefully considered before using passive systems, since if the bridge is located over deep flexible alluvium, predominant frequencies of the ground-motions will likely occur in the long run. In any case, structures designed with base isolation systems need to deform in a controlled manner even if an earthquake greater than the design earthquake occurs.

1.4 Main Base Isolation Systems Used in Canada

Many seismic isolation devices exist, such as elastomeric bearings, sliding bearings and roller bearings. According to Skinner et al. (1993), a total of 255 isolated bridges existed in the world as of 1993. In Canada, two basic types of isolators for bridges are used; elastomeric and sliding bearings. Vancouver and other western cities of Canada have started using these systems in 1990 (Matson & Buckland, 2009). The province of Quebec only started employing them in 2002 (Guizani, 2007).

1.4.1 Elastomeric Base Isolation Systems

Elastomeric base isolators are simply elastomeric bearings with mechanical energy-dissipating devices. Three different types of elastomeric bearings exist:

1) Low-damping natural or synthetic rubber bearing
2) High-damping natural rubber bearing
3) Lead core rubber bearing (LRB)

The most flexible base isolation device used for bridges is the lead core elastomeric isolation bearing. Hundreds of bridges worldwide have used LRBs for retrofit or in new designs (Chen & Duan, 2000). Figure 1.4 illustrates the device.

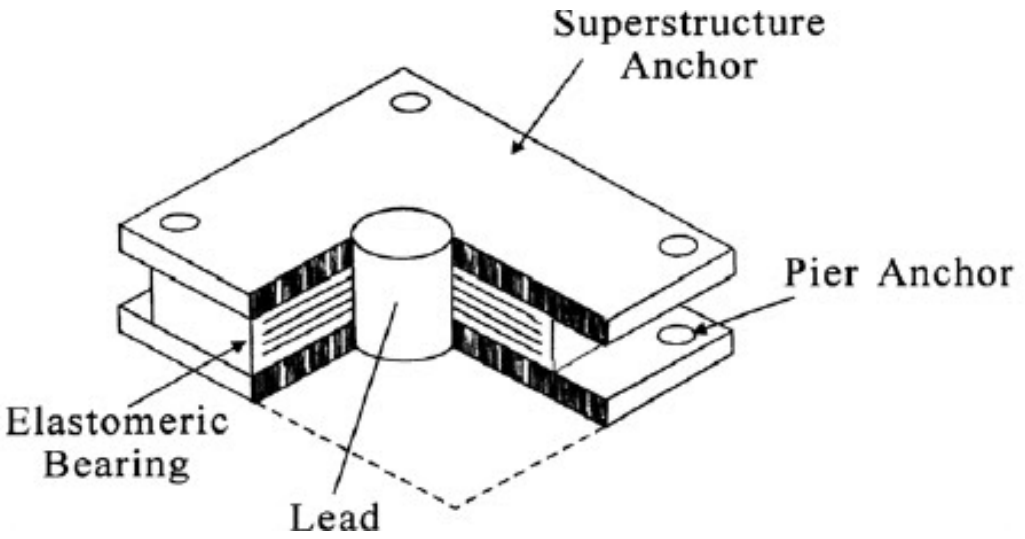

Figure 1.4: Lead core rubber bearing (Milne, Ritchie, & Karihaloo, 2003)

Elastomeric isolators are generally cylindrical or rectangular, and are mostly made of rubber. Once properly installed on bridge piers or abutments, the elastomeric bearings allow the superstructure to translate and rotate, but resist loads in the longitudinal, transverse and vertical directions. In order to do so, the bearings must be stiff enough to resist the vertical loads, but relatively flexible to resist lateral loads. LRBs are laminated elastomeric bearings manufactured from layers of rubber sandwiched together with horizontal steel plates and a lead plug at its core. The layers of rubber provide the lateral flexibility the isolator requires. The steel plates increase the vertical stiffness of the isolator and improve its stability under lateral loading. Fundamentally, the maximum allowable lateral displacement and period of vibration are controlled by the total rubber thickness. As for the lead core, it acts as the isolator's energy dissipation device and dissipates the energy during an earthquake. By acting as a single unit, the LRB's lead plug experiences the same deformation as the rubber, but converts the kinetic energy into heat and dampens the structure's vibrations. Lead is known to have excellent elastic-

plastic behaviour with good fatigue properties since it has a high initial shear stiffness and relatively low shear yielding strength. These characteristics are shown in Figure 1.5.

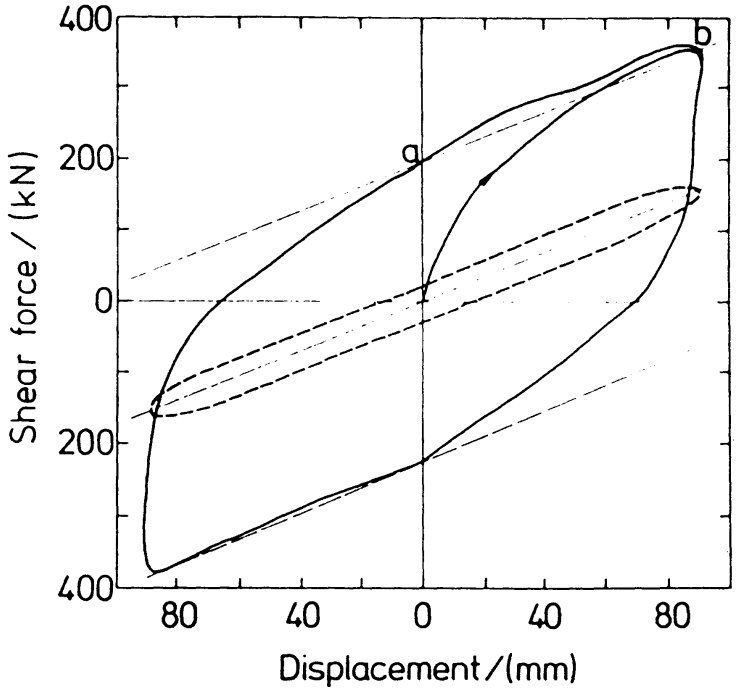

Figure 1.5: Hysteresis loops of a typical LRB (Chen & Duan, 2000)

The horizontal stiffness K of an elastomeric isolator is a function of its bearing area A, shear modulus G, and height h.

$$K = \frac{G \times A}{h} \tag{1.1}$$

The period of vibration of the isolator T is a function of the mass of the supported structure M, and its horizontal stiffness K.

$$T = 2\pi\sqrt{\frac{M}{K}} \tag{1.2}$$

Many limitations exist for LRBs. In fact, LRBs are sensitive to thermal changes. The colder the temperature, the stiffer the elastomeric bearing gets, which consequently

reduces the seismic period of the isolated structure. Also, as the LRBs deform laterally, the vertical load they can resist consequently decreases (Guizani, 2007).

1.4.2 Sliding Base Isolation Systems

Sliding bearings act differently than elastomeric bearings to isolate the superstructure of a bridge from its substructure. During earthquake ground-motions, sliding-type isolation bearings allow the superstructure elements to slide on a low friction surface typically made from stainless steel-Polytetrafluoroethylene (PTFE). Friction between the sliding surfaces dissipates energy and the maximum friction limits the transfer of shear across the isolation boundary. There are two basic types of sliding bearings:

1) Flat sliding bearing
2) Spherical sliding bearing or friction pendulum isolation bearing

Friction pendulum isolation (FPI) bearings naturally self-centre themselves after ground shaking or any displacement demand, since its sliding surface is curved such that the deadweight of the bridge will facilitate its superstructure to re-centre. Flat sliding bearings, on the other hand, need a mechanical system for re-centring, such as spring elements. This complicates immensely its anticipated response. For this reason, sliding base isolation systems studied in this thesis are represented only by Earthquake Protection Systems (EPS) as FPI bearings (Earthquake Protection Systems, 2003).

FPI bearings utilize the characteristics of a simple pendulum to lengthen the natural period of vibration of the isolated structure, and as a result, reduce the earthquake

forces applied. Basically, they consist of an articulated friction slider with a PTFE surface bearing material and a treated spherical concave surface of hard-dense chrome over steel. The concave surface may face up or down without changing the operational capabilities of the bearing. Figure 1.6 illustrates a section view of the isolator with its concave surface facing up.

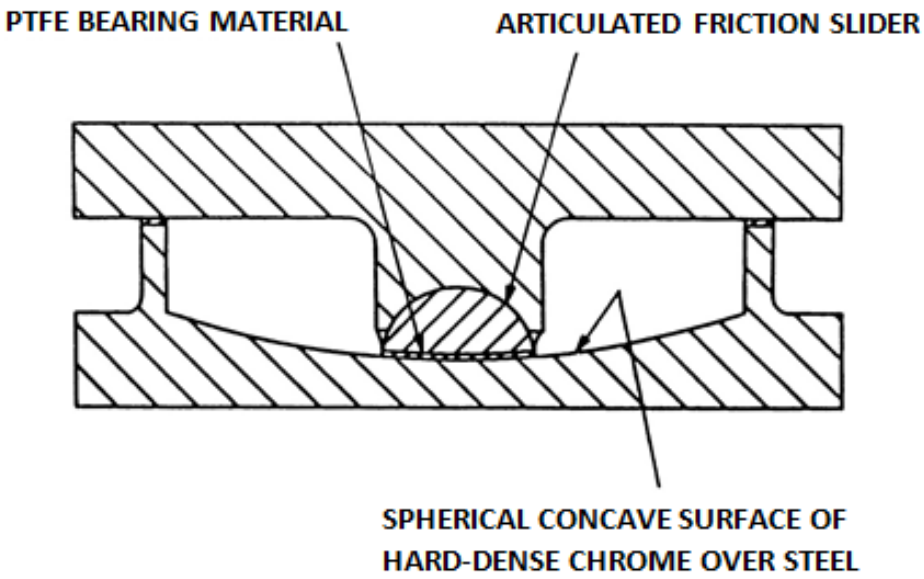

Figure 1.6: Typical FPI bearing (Chen & Duan, 2000)

The isolator is very practical in design since its concave surface and the slider's surface have the same radius of curvature and a relatively uniform pressure under vertical loads. Also, its radius is independent of the mass of the supported structure, and the maximum design displacement ultimately controls the size of the bearing. Finally, the centre of stiffness of the bearings always coincides with the centre of mass of the supported structure, which minimizes torsion-motions of the bridge.

The lateral restoring stiffness of a FPI bearing K is a function of the weight of the supported structure W, and the radius of curvature of the concave surface R.

$$K = \frac{W}{R} \tag{1.3}$$

The isolator's period of vibration T is a function of the radius of curvature of the concave surface R.

$$T = 2\pi\sqrt{\frac{R}{g}} \tag{1.4}$$

where

g = the acceleration due to gravity

The above-defined period does not change for light or heavy structures, and regardless of whether the structure's weight changes over time, which represents a great advantage. Also, the reliability of the dynamic and sliding properties of FPI bearings have been proven through numerous tests over the years. Indeed, experimental hysteretic loops generated from tests on full-size bearings have demonstrated an ideal bi-linear response of the FPI bearings with no degradation under repeated cyclic loading at different conditions. Figure 1.7 shows test results for 10 cycles at 1.2x design displacement.

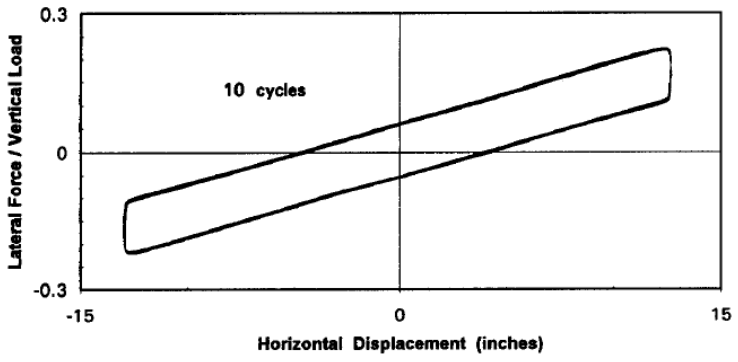

Figure 1.7: FPI bearing's hysteretic loop (Earthquake Protection Systems, 2003)

Like elastomeric bearings, FPI bearings are sensitive to thermal changes. As temperature rises, friction decreases. Vice-versa, when temperature decreases, friction increases. On the other hand, bearing dynamic stiffness and period are not affected by temperature. Lastly, the isolator's effective stiffness and period are slightly affected by temperature due to the friction coefficient change. Figure 1.8 shows the effect of temperature on dynamic friction.

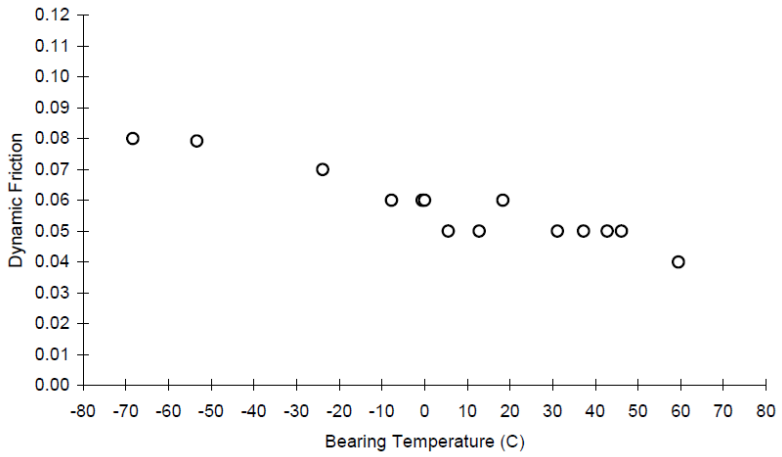

Figure 1.8: Effect of temperature on dynamic friction of FPI bearings (Earthquake Protection Systems, 2003)

Finally, it is important to note that FPI systems will only behave rigidly if the lateral loads applied to the isolator are less than its friction force. In the case of an earthquake loading, the lateral force will exceed the isolator's friction force, and the isolated structure will respond at its isolated period (Chen & Duan, 2000).

1.5 Objectives and Thesis Layout

The specific objectives of this thesis are:

1) To present the calculation methods recommended by the CHBDC CSA-S6-06 to determine the longitudinal thermal and seismic displacements of base isolators in bridges.
2) To suggest different ways to combine these displacements in order to have a more realistic design approach with updated ground-motion relations.

This study is divided into four chapters:

Chapter 2 provides a summary of international thermal and seismic bridge code provisions.

Chapter 3 explains different load combination methods used to develop a thermal and seismic displacement combination formula for base isolated bridges.

Chapter 4 presents the results of two base isolated bridges analyzed under Montreal and Vancouver's thermal and seismic provisions. New seismic models are utilized.

Chapter 5 discusses the results of the analyses.

Chapter 2 International Base Isolation Design Provisions

This chapter describes how thermal displacements are calculated according to the CHBDC CSA-S6-06. Seismic displacements of base isolated bridges are also presented for different international bridge standards. The latter portion of this chapter offers a summary illustrating how international bridge codes combine thermal and seismic displacements to ensure adequate structural clearance for the structure.

2.1 CHBDC CSA-S6

2.1.1 CSA-S6-06 Thermal Deformation Design

Temperature changes deform the constituent materials of a bridge. Expansion joints and bearings must therefore accommodate superstructure movement. Traditionally, only the overall longitudinal displacement caused by temperature was taken into account in the CHBDC. Recent findings, however, show that bridges deform in different directions as a function of climatic conditions.

This thesis only addresses thermal longitudinal displacements of straight bridges for simplicity. They are determined by specifying an effective bridge temperature range, which depends on the location, geometry, and type of superstructure. Localized effective temperatures may be assessed for bridges when factors such as altitude, exposure of the structure, and orientation to the sun are known. Due to thermal effects, bridges that are straight in plan usually deform along their centreline. Curved bridges deform

longitudinally along their centreline, and transversely perpendicular to their longitudinal centreline. Three different bridge types are considered when calculating the effects of temperature changes:

1) Type A: steel bridge structures
2) Type B: steel beam, box, or deck truss structures with concrete decks
3) Type C: concrete bridge structures

They are categorized in the CHBDC CSA-S6-06 based on their thermal conductivity. Wood structures are not required to be analyzed for temperature effects according to the code since they appear to perform satisfactorily.

To calculate the thermal displacements of regular bridges in the longitudinal direction, $\Delta_{thermal}$, the CHBDC CSA-S6-06 recommends the following equation:

$$\Delta_{thermal} = \alpha \times L \times \Delta \times T \qquad (2.1)$$

where

α = thermal coefficient of bridge superstructure, $^{0}C^{-1}$

L = length of member subjected to deformation, mm

ΔT = temperature differential after onsite installation, ^{0}C

Thermal coefficients are provided in the code, such as clause 8.4.1.3 of the CSA-S6-06 which states that the thermal coefficient of linear expansion of concrete shall be taken as 10 x $10^{-6}/^{o}C$. Also, temperature differentials are defined in the code by determining the maximum and minimum mean daily bridge effective temperatures. Figures 2.1 and 2.2 represent the climatic database of Section 3 of the CHBDC CSA-S6-06.

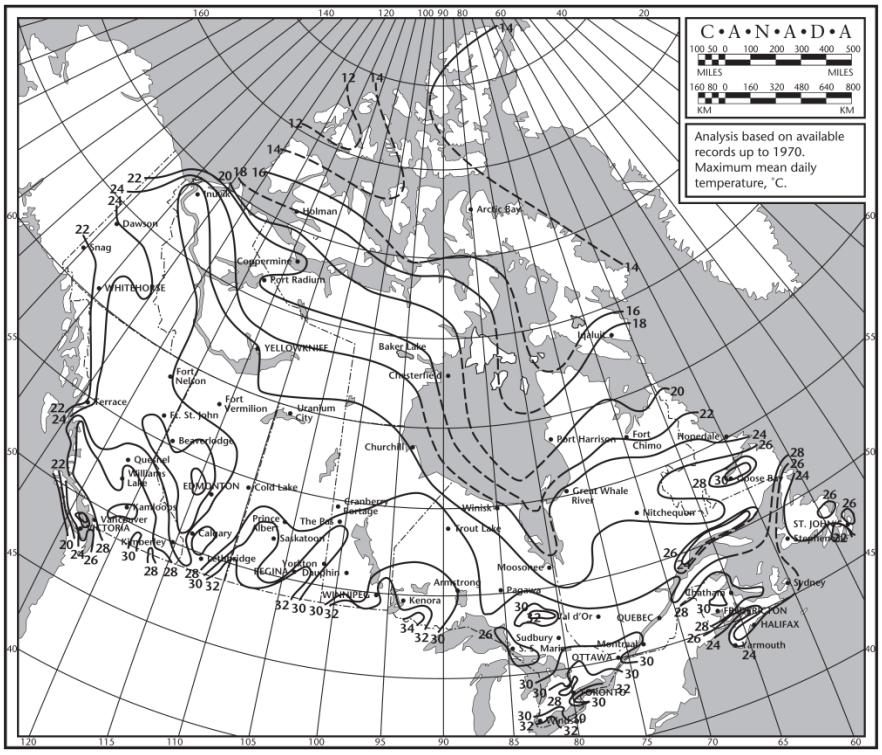

Figure 2.1: Maximum mean daily temperature (CSA, 2006a)

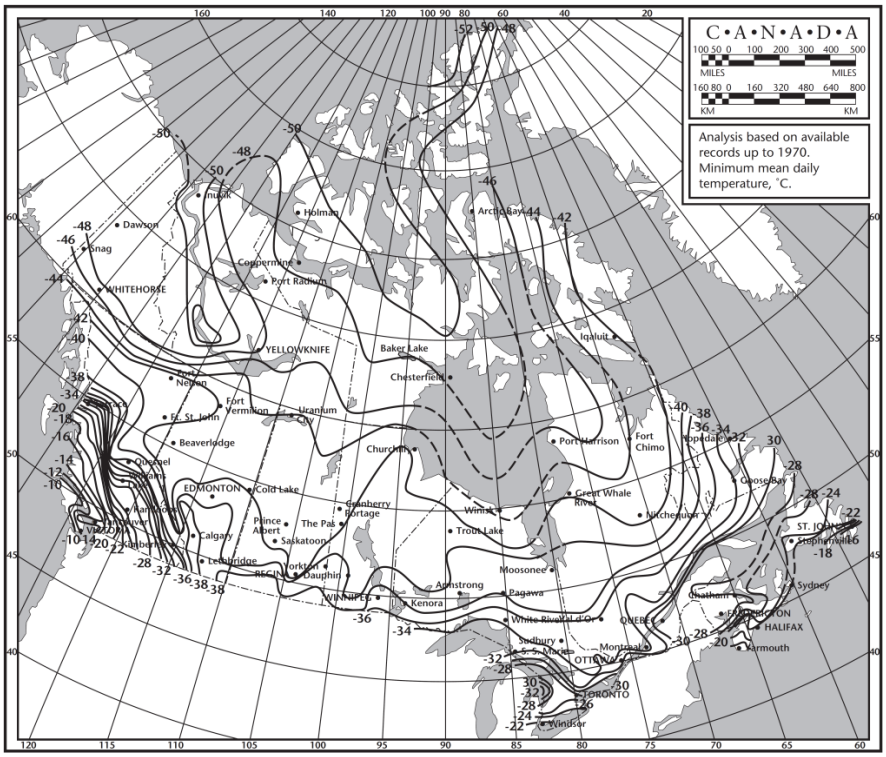

Figure 2.2: Minimum mean daily temperature (CSA, 2006a)

Once the maximum and minimum mean daily temperatures are determined, they must be modified to reflect the bridge's effective temperature range as specified in Table 2.1 and Figure 2.3.

Table 2.1: Maximum and minimum effective temperatures (CSA, 2006a)

Superstructure type	Maximum effective temperature	Minimum effective temperature
A	25 °C above maximum mean daily temperature	15 °C below minimum mean daily temperature
B	20 °C above maximum mean daily temperature	5 °C below minimum mean daily temperature
C	10 °C above maximum mean daily temperature	5 °C below minimum mean daily temperature

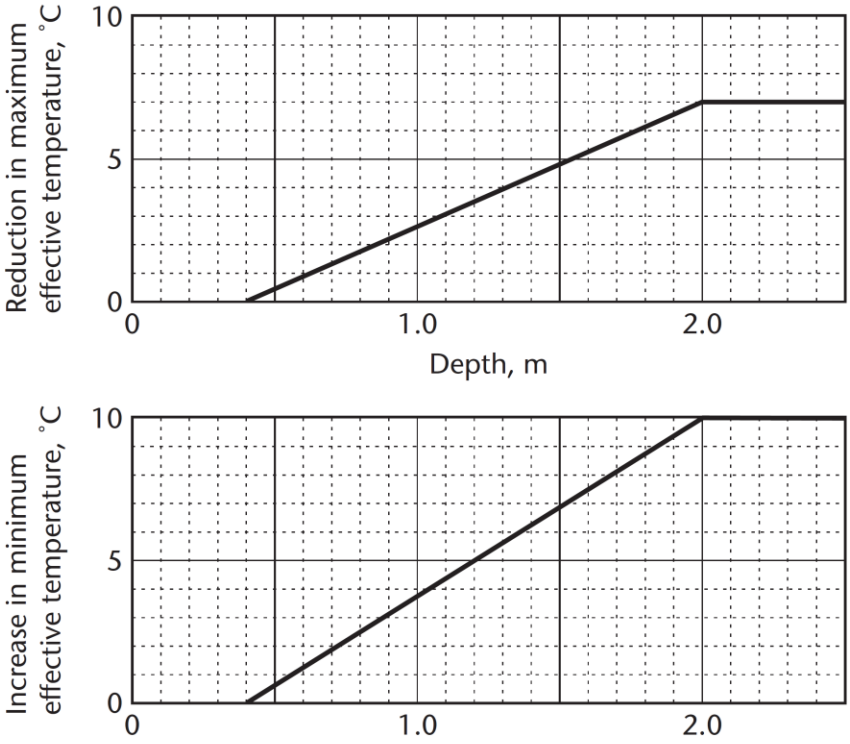

Figure 2.3: Modifications to maximum and minimum effective temperatures (CSA, 2006a)

With an assumed effective construction temperature of 15 ^{0}C, ΔT can be defined, and expansion and contraction calculations can be performed. Thermal displacements are calculated using the same equation in other international codes. However, thermal coefficients of materials may vary slightly from code to code.

2.1.2 CSA-S6-06 Seismic Base Isolation Design

Canada collaborates closely with the United States of America when it comes to seismic research. The CHBDC seismic design provisions are therefore very similar to those of AASHTO. To calculate the design seismic displacements of base isolated bridges, the CHBDC CSA-S6-06 recommends the uniform-load/single-mode spectral analysis, multi-mode spectral analysis, and time-history analysis. Single and multimodal methods of analysis may be used for seismic isolation design, since the energy dissipation of base isolation devices can be considered in terms of equivalent viscous damping, and their stiffness can be treated as an effective linear stiffness. The minimum design requirements and method of analysis are determined by the seismic performance zone of the bridge (CSA, 2006b).

This thesis covers the uniform-load/single-mode spectral analysis. According to this analysis method, the design seismic displacement is derived from the elastic seismic response coefficient for base isolation systems, C'$_{sm}$. The equation for C'$_{sm}$ is given below and does not take into consideration the importance factor, since all isolated bridges are designed to perform equally for the design earthquake.

$$C'sm = \frac{A \times Si}{Te \times B} \leq \frac{2.5A}{B} \qquad (2.2)$$

C'_{sm} is a dimensionless design coefficient, A is the zonal acceleration ratio, S_i is the site coefficient, T_e is the period of the seismically isolated structure, and B is a coefficient related to the effective damping of the isolated bridge. When C'_{sm} is multiplied by the acceleration due to gravity, g, a spectral acceleration, S_a, is created.

$$S_a = \frac{(A \times Si)}{Te \times B} \times g \tag{2.3}$$

Once S_a is produced, the spectral displacement across the isolation bearing, S_D, can be determined by the relationship

$$S_D = \frac{Sa}{\omega^2} \tag{2.4}$$

where ω is the circular natural frequency and is equal to $2\pi / T_e$. Therefore,

$$\Delta_{seismic} = S_D = \frac{(250 \times A \times Si \times Te)}{B} \tag{2.5}$$

The zonal acceleration ratio, A, corresponds to an event with 10% probability of exceedance in 50 years, which is equivalent to a 15% probability of exceedance in 75 years with a minimum value of 0.1 (CSA, 2006a). A and S_i coefficients are provided in the CHBDC CSA-S6-06, and the damping coefficient of the isolated bridge, B, is limited to 1.7 in equation 2.5. Table 2.2 represents the relationship between the equivalent viscous damping, β, and the damping coefficient, B.

Table 2.2: Damping coefficient, B (CSA, 2006a)

Equivalent viscous damping, β (% of critical)	**Damping coefficient, B**
≤ 2	0.8
5	1
10	1.2
20	1.5
30	1.7
40	1.9
50	2

T_e is determined by the following expression,

$$T_e = 2\pi\sqrt{\frac{W}{\sum Keff \times g}} \quad (2.6)$$

where

W = dead load of the superstructure segment supported by isolation bearings

$\sum K_{eff}$ = sum of the effective linear stiffnesses of all bearings and substructures supporting the superstructure segment, calculated at the seismic displacement across the isolation bearings

However, this thesis uses newly developed earthquake ground-motion relations for 5% damped horizontal spectral parameters with 2% probability of exceedance in 50 years instead of the CHBDC CSA-S6-06 zonal acceleration ratios, A, with a return period of 475 years. Consequently, for the purpose of this thesis, S_D can be obtained through equation 2.4 as such

$$\Delta_{seismic} = S_D = \frac{Sa}{\omega^2} = \frac{(250 \times Sa \times Si \times Te^2)}{B} \quad (2.5)$$

Finally, the seismic design displacement, S_D, is the maximum seismic displacement calculated in the two orthogonal directions of the isolator (CSA, 2006b).

2.2 Eurocode 8 Seismic Base Isolation Design

The base isolated bridge provisions of the 2003 edition of the Eurocode 8 recommend three very similar methods of analysis to the CHBDC CSA-S6-06, which are:

1) Fundamental mode spectrum analysis
2) Multi-mode spectrum analysis
3) Time-history non-linear analysis

The fundamental mode spectrum analysis method presented in this thesis calculates the design seismic displacement almost exactly as the CHBDC-CSA-S6-06 single-mode spectral analysis. For instance, not only does the analysis described in this thesis consider the superstructure of the bridge to behave as a single degree of freedom system, but it also uses:

3) Effective stiffness of the isolation system, K_{eff}
4) Effective damping of the isolation system, ξ_{eff}
5) Mass of the superstructure, W_d/g
6) Spectral acceleration corresponding to the effective period, T_{eff}, with

$\eta_{eff} = \eta(\xi_{eff})S_e(T_{eff}, \eta_{eff})$

where

η_{eff} = damping correction factor

Given all of the above information, however, the Eurocode 8 preliminary design for seismic displacement d_{dc} is different from the one presented in the latest version of the CHBDC, and is defined in Table 2.3.

Table 2.3: Eurocode 8 design seismic displacement d_{dc} (BSI, 2003)

$\mathbf{T_{eff}}$	$\frac{\boldsymbol{Smax}}{\boldsymbol{g}}$	$\mathbf{d_{dc}}$
$T_C \leq T_{eff} < T_D$	$2{,}5\,\frac{TC}{Teff} S\eta eff \times \alpha \times g$	$\frac{Teff}{Tc} dc$
$T_D \leq T_{eff}$	$2{,}5\,\frac{TC \times TD}{Teff^2} S\eta eff \times \alpha \times g$	$\frac{TD}{TC} dc$

where

$$d_c = 0.625\,\frac{g}{\pi^2} ag \times S\eta eff \times Tc^2 \qquad (2.7)$$

g = acceleration coefficient

a_g = design ground acceleration on rock corresponding to the importance category of the bridge

S = soil parameter

T_c = period of the fundamental mode of vibration for the direction under consideration, s

S and T are parameters of the applicable design spectrum and specific soil condition, and are provided in part 1 of the Eurocode 8. Also, it is important to note that, unlike the CHBDC CSA-S6-06, the design ground acceleration on rock corresponding to a design seismic event with a reference return period of 475 years is multiplied by the importance factor, γ_{IS}, of the bridge in equation 2.7. Eurocode 8 recommends 1.50 to be selected as γ_{IS} for lifeline bridges (BSI, 2003).

2.3 New Zealand Bridge Manual Seismic Base Isolation Design

In New Zealand, engineers started using base isolation devices for bridges in the early 1970s. In fact, in 1973, the Motu Bridge was erected and was the first bridge to use seismic isolators in the country. In 1995, a total of 50 bridges were built utilizing such isolators. In most cases, LRBs were employed. (Park & Blakeley, 1978). According to the 2004 version of the New Zealand Transport Agency (NZTA) Bridge Manual, seismic displacements can also be calculated by using the single-mode spectrum analysis method. As long as a bridge is recognized as a single degree of freedom oscillator, the maximum seismic displacement, Δ, of the centre of mass may be determined by using equation 2.8 (NZTA, 2004).

$$\Delta = \mu \times C_{\mu} \times g \times Z \times R \times S_P \times T^2/(4\Pi^2) \qquad (2.8)$$

where

μ = displacement ductility factor

C_{μ} = basic acceleration coefficient according to the value of T and the site subsoil category

g = acceleration due to gravity

Z = zone factor

R = risk factor

S_P = structural performance factor

T = fundamental natural period, s

However, as can be seen from the parameters of equation 2.8, New Zealand accounts like the Eurocode 8 for the risk or importance factor of the bridge in its

preliminary seismic displacement calculation. Figure 2.4 illustrates how the 2004 NZTA Bridge Manual provides C_μ values for very stiff soil sites.

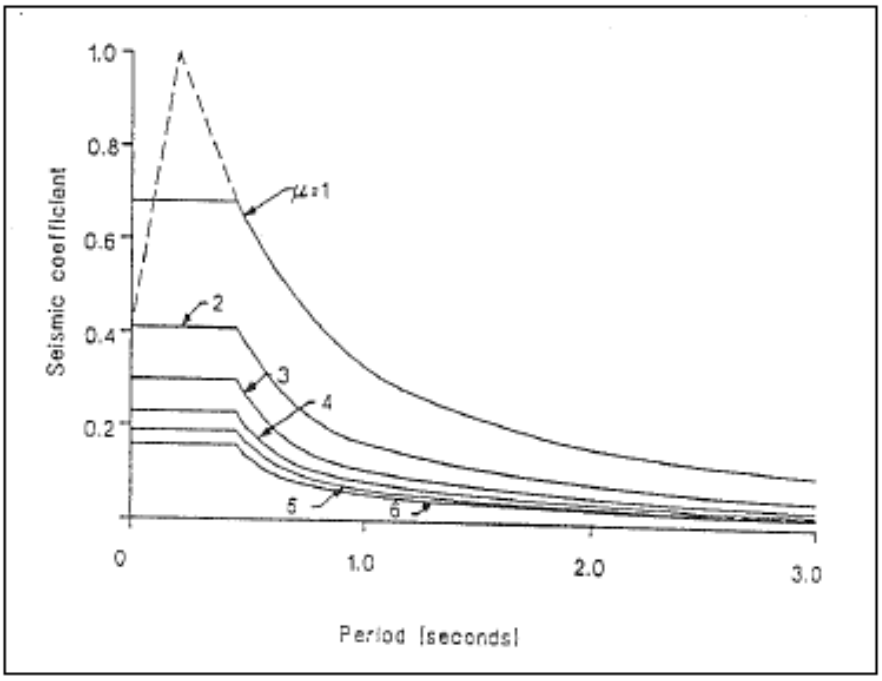

Period, T Seconds	Structural ductility factor, μ					
	1.0	2.0	3.0	4.0	5.0	6.0
0	0.40 0.68	0.41	0.30	0.23	0.19	0.16
0.2	1.00	0.41	0.30	0.23	0.19	0.16
0.45	0.68	0.41	0.30	0.23	0.19	0.16
0.5	0.63	0.37	0.26	0.20	0.16	0.14
0.6	0.55	0.30	0.20	0.15	0.13	0.10
0.7	0.48	0.24	0.16	0.12	0.10	0.082
0.8	0.42	0.21	0.14	0.11	0.084	0.071
0.9	0.37	0.19	0.12	0.093	0.074	0.063
1.0	0.33	0.17	0.11	0.083	0.066	0.056
1.5	0.23	0.12	0.076	0.058	0.046	0.039
2.0	0.17	0.085	0.056	0.043	0.034	0.029
2.5	0.13	0.065	0.043	0.033	0.026	0.022
3.0	0.11	0.055	0.036	0.028	0.022	0.019

Figure 2.4: New Zealand's basic seismic hazard acceleration coefficient, C_μ, for very stiff soil sites (NZTA, 2004)

2.4 Summary of International Bridge Base Isolation Design Provisions for Combination of Thermal and Seismic Displacements

In Canada, thermal movements must be considered when horizontal deflections of seismic isolators are determined. However, the CHBDC CSA-S6-06 does not recommend any load combination methods. Engineering judgement is simply advised (CSA, 2006b). The Americans follow the same design guideline (AASHTO, 2004).

Nevertheless, in the British Columbia Bridge Standards and Procedures Manual, which is a Supplement to the CHBDC CSA-S6-06, Clause 4.10.7 clearly states: "40% of the thermal deformation demands shall be combined with deformation demands from the base isolation system" (BC Ministry of Transportation, 2010).

Similarly, the Eurocode 8 Bridge Standards recommend that 50% of the thermal deformations be combined with the design seismic displacements of each isolator unit in each direction. Also, offset displacements potentially generated by permanent actions and long-term deformations, such as concrete shrinkage and creep, must be combined to calculate the design total maximum displacements of each base isolator (BSI, 2003).

Finally, the NZTA Bridge Manual also provides specific guidelines for bridge engineers to combine thermal and seismic displacements of base isolation systems. Clause 5.6.1 requires that "long term shortening effects and one third of the temperature induced movement from the median temperature position shall be taken into account" (NZTA, 2004).

Table 2.4 summarizes the recommended design combination equations for both thermal and seismic displacements of bridge isolators for each previously presented bridge manual.

Table 2.4: International combination formulas for base isolators depending on seismic and thermal parameters

National Bridge Design Code	**Combination of seismic and thermal displacement**	**Clause**
CSA-S6-06 & AASHTO 2004	None	-
British Columbia Supplement to CHBDC CSA-S6-06	$\Delta_{seismic} + 40\%\Delta_{thermal}$	4.10.7
2004 NZTA Bridge Manual	$\Delta_{seismic} + 33.3\%\Delta_{thermal}$	5.6.1
2003 Eurocode 8	$\Delta_{seismic} + 50\%\Delta_{thermal}$	7.6.2

Chapter 3 Load Combination Methods

Most applied loads on structures, particularly bridge structures, are random and dynamic in nature, and may also stem from common or related sources. To achieve optimum design, the combination of load effects must therefore be carefully studied. Several load combination formulas and theories currently exist and have proven to increase the safety and performance of structures over their useful service lifetime. In this chapter, the total probability theorem, Turkstra's rule and Wen's load coincidence method are considered.

3.1 Total Probability Theorem

The law of total probability is a fundamental rule in probability theory and is used to determine the probability that an event B will occur even though only the conditional relationships of the event are given to a set of mutually exclusive and collectively exhaustive events (Augustini, Baratta, & Casciati, 1984).

Therefore, according to the probability theorem:

$$P(B) = \sum_{i=1}^{n} [P(B \mid A_i) \times P(A_i)] \tag{3.1}$$

where

A_i = single events, which are mutually exclusive and collectively exhaustive

In this thesis, the total probability theorem is utilized to combine thermal and seismic displacements for the design of base isolated bridges in Canada. The methodology consists of following the next few steps:

Step 1: Derive the probability distribution function for the temperature differentials for the bridge.

Step 2: Discretize the range of temperature differentials using N equal increments, ΔT.

Step 3: For each ΔT_i, add the thermal displacement to the seismic hazard curve for total displacements. Determine the return period, λ_i, which will provide the same displacement as $\Delta_{seismic}$.

Step 4: Calculate the average return period corresponding to the seismic displacement using the total probability theorem.

$1/RP_{average} = \sum_{i=1}^{N}(\lambda i \times Pi)$

Step 5: If $RP_{average}$ = 2475 years, stop.

Otherwise, reduce RP and repeat steps 2, 3 and 4 until the condition is met.

Step 6: Once $RP_{average}$ = 2475 years, the percentage of thermal displacement combined with the maximum seismic displacement can be determined as follows:

$$\Delta_{thermal\ ave}/\Delta_{thermal\ max} = (\Delta_{seismic\ @\ \lambda 2} - \Delta_{seismic\ @\ 1/2475})/\Delta_{thermal\ max} = \%\Delta_{thermal} \quad (3.2)$$

3.2 Turkstra's Rule

Turkstra's rule is a simple deterministic method which combines the effect of extreme loads on structures based on the theory of structural reliability. Basically, the rule is an over-simplification of Ferry Borges-Castanheta model for load combination (Borges & Castanheta, 1971), and takes into consideration the intensity of the effect of each random time-varying load. When applying Turkstra's rule, one must design for the maximum of one load (Load 1) plus the value of the other load (Load 2) that will occur when the maximum value of the first load (Load 1) is on. Usually, when a load is not equal to its maximum value, it is taken at its mean value (Ghosn, Moses, & Wang, 2003). Turkstra's rule is consequently expressed as follows:

$$X_{\max,\,T} = \max\begin{Bmatrix}[\max(x_1) + \bar{x}_2]\\ [\bar{x}_1 + \max(x_2)]\end{Bmatrix} \tag{3.3}$$

where

$X_{\max,\,T}$ = the maximum value for the combined load effects in a period of time T

x_1 = load 1

$\bar{x}_1$ = mean value of load 1

x_2 = load 2

$\bar{x}_2$ = mean value of load 2

Turkstra's rule was also used in this thesis to combine thermal and seismic displacements for the design of base isolated bridges in Canada. However, this simplistic method can provide inconsistent results at times (Melchers, 1999). Essentially, in this

thesis, Turkstra's rule is divided into two procedures to determine the $\%\Delta_{thermal}$ to combine with the design $\Delta_{seismic}$ of the base isolation system:

1) If Seismic Displacement Controls ($\Delta_{seismic} > \Delta_{thermal}$)

$\Delta_{seismic\ max} + \Delta_{thermal\ ave} = \Delta_{tot}$

$\%\Delta_{thermal} = (\Delta_{thermal\ ave})/ (\Delta_{thermal\ max})$

2) If Thermal Displacement Controls ($\Delta_{thermal} > \Delta_{seismic}$)

$\Delta_{thermal\ max} + \Delta_{seismic\ ave} = \Delta_{tot} = \Delta_{seismic\ max} + \Delta_{thermal\ ave}$

$\%\Delta_{thermal} = ((\Delta_{thermal\ max} + \Delta_{seismic\ ave}) - \Delta_{seismic\ max})/(\Delta_{thermal\ max})$

It is important to remember that when designing for an earthquake with a probability of occurrence of 2% in 50 years, the earthquake can occur randomly at any point in time during the design life of the bridge. However, to calculate the maximum thermal displacements, the maximum effective temperature differentials generally occur in a small timeframe roughly equal to 10% of a year. Therefore, if an engineer wants to design its structure to resist both the maximum probable thermal displacement, $\Delta_{thermal\ max}$, and a constant annual level of seismic risk or an average seismic displacement, $\Delta_{seismic\ ave}$, only 10% of a year may be considered in design practice. In other words, the maximum seismic event must be decreased by this same amount to produce $\Delta_{seismic\ ave}$.

3.3 Wen's Load Coincidence Method

Wen's load coincidence method is a complex load combination method which can be used for both linear and nonlinear combinations of processes. Dynamic fluctuations are also covered in this reliable and accurate method. However, unlike the two previously

presented methods, it does not assume independence between two different load cases (Ghosn, Moses, & Wang, 2003).

The following equation represents Wen's load coincidence method:

$$P(E,T) \approx 1 - \left\{ \exp\left\{ -\left[\sum_{i=1}^{n} \lambda_i p_i + \sum_{i-1}^{n-1} \sum_{j=i+1}^{n} \lambda_{ij} p_{ij} + \cdots \right] T \right\} \right\} \tag{3.4}$$

where

P(E, T) = the probability of reaching limit state E in a time period T

n = the total number of load types each designated by the subscripts *i* and *j*

λ_i = the rate of occurrence of load type *i*

p_i = the probability of failure given the occurrence of load type *i* only

λ_{ij} = the rate of occurrence of load types *i* and *j* simultaneously

p_{ij} = the probability of failure given the occurrence of load types *i* and *j* simultaneously

The mathematical formulation of Wen's method respects a Poisson process which assumes that limit states of different events are independent. This process can be applied to many different load combinations depending on the nature of the load and its structural behaviour. A limit state may be established as the probability of failure or the probability of exceeding a response level of different events (Elsevier B.V., 1983). Table 3.1 illustrates the classification system of all possible combinations of load effects.

Table 3.1: Classification of combination of load effects (Elsevier B.V., 1983)

Load type	**Structure response**	**Limit state**
Static (macro-scale)	Linear	Linear
		Nonlinear
	Nonlinear	Nonlinear
Dynamic (macro- and micro-scale)	Linear	Linear
		Nonlinear
	Nonlinear	Nonlinear

Finally, Wen's method is valid in situations where the intensities of the loads may be represented by pulse-like functions of time for very short duration. Since thermal loads do not meet this criterion, Wen's load coincidence method was not used in this thesis.

Chapter 4 Base Isolation System Analyses and Results

The Madrid Bridge and the A30 Bridge over the St-Lawrence River are analyzed in this chapter according to basic CHBDC CSA-S6-06 thermal and seismic design methods. These two Canadian bridges are equipped with seismic base isolation and are analyzed with new seismic hazard models with revised attenuation factors by Atkinson and Boore 2006, and by Atkinson and Goda 2010. Only data for Montreal and Vancouver are utilized in this chapter. Also, LRB and FPI bearings are treated individually for both bridges, and the effects of climate on performance are considered. Finally, the objective of this chapter is to present the results generated from the total probability theorem and Turkstra's rule when thermal and seismic displacements of base isolators are combined.

4.1 Seismic Hazard Models Used for Analyses

Currently, the CHBDC CSA-S6-06 seismic design requirements are based on Canada's 3rd generation maps and the NBCC 1995, with a probabilistic assessment at 0.0021 p.a. for both peak ground acceleration (PGA) and velocity (PGV). Also, the code uses a seismic zoning map containing seven distinct zones based on a statistical analysis of historical earthquakes records, and assigns 0.20 g as the zonal acceleration ratio for Montreal and Vancouver even though they have significantly different ground-motion characteristics (CSA, 2006a). This zoning system often leads to under or overdesigns.

The hazard models utilized in this thesis are the ones presented by Atkinson and Boore (2006) and Atkinson and Goda (2010). They are based on the 4th generation

seismic hazard maps developed by the Geological Survey of Canada (GSC) for the NBCC 2005, and consider aleatory and epistemic uncertainties. The former is due to randomness in progress and cannot be reduced by collecting additional information, and the latter is due to uncertainty in knowledge and can be reduced by collecting additional information (Natural Resources Canada, 2011). Also, the new earthquake ground-motion relations are for 5% damped horizontal spectral parameters with 2% probability of exceedance in 50 years. Increasing the return period from 475 to 2,475 years increases the ground-motions by a factor of 2±0.3, and improves earthquake-resistant design. As can be seen in Figure 4.1, eastern cities of Canada generally are associated with a larger increase than western cities.

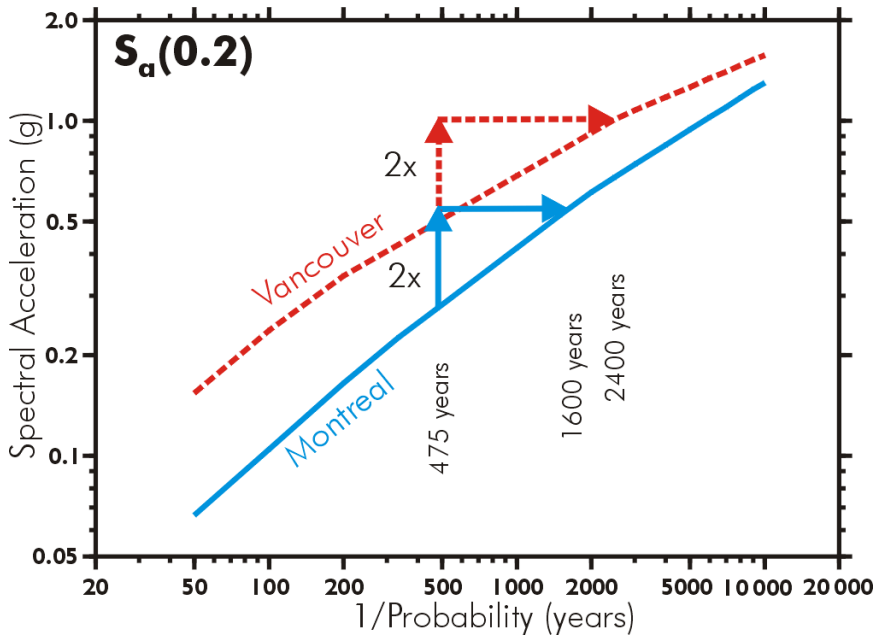

Figure 4.1: Montreal and Vancouver's hazard curves for a period of 0.2 seconds (Natural Resources Canada, 2011)

Atkinson and Boore's 2006 earthquake ground-motion relations for eastern North America (AB06) are based on stochastic finite-fault sources and are derived from observed ground-motion data. Their new ground-motion prediction equations (GMPEs) are similar to the ones they developed in 1995, which were based on a stochastic point-source model. A decade later, the main difference between the two models is that new seismicity rates having frequency amplitudes larger or equal to 5 Hz are smaller than the ones predicted earlier, because of a slightly lower average stress parameter and steeper near-source attenuation (GeoScienceWorld, 2006). Figure 4.2 and Figure 4.3 illustrate the hazard curves constructed for Montreal's site class A and C (NEHRP) respectively.

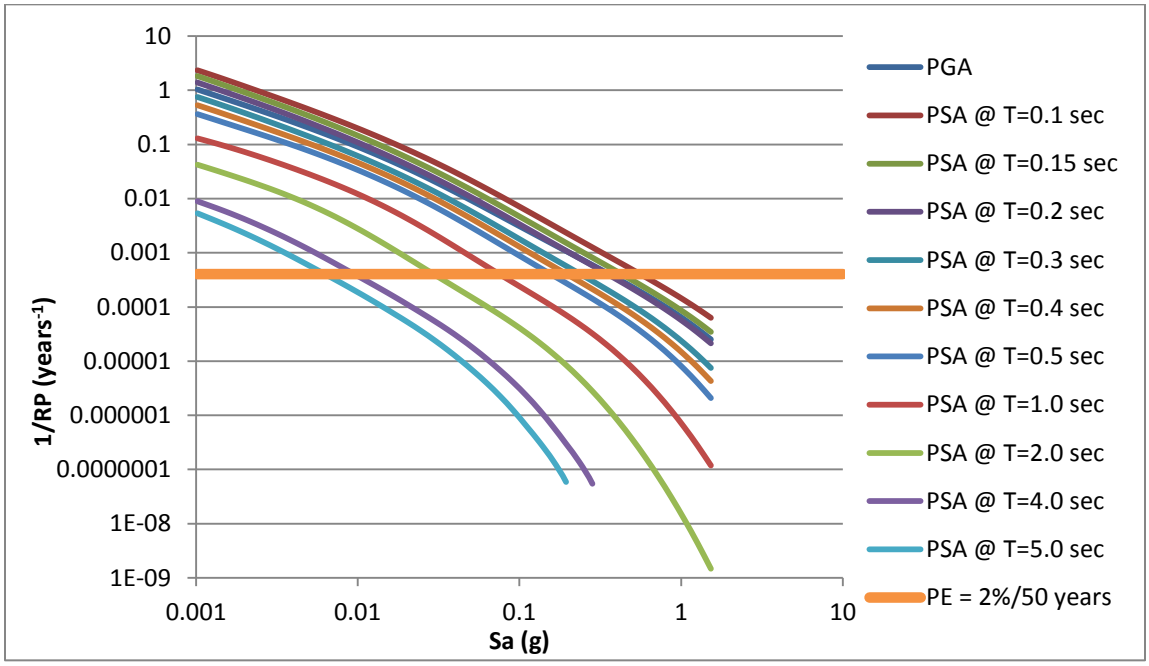

Figure 4.2: AB06 Montreal site class A hazard curves

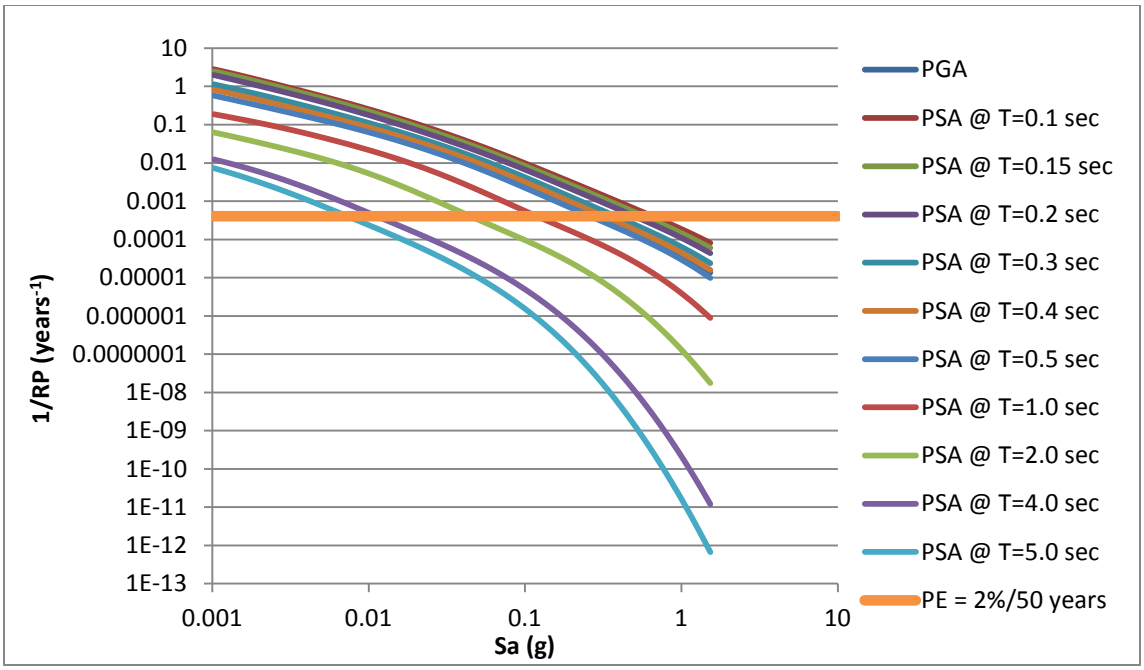

Figure 4.3: AB06 Montreal site class C hazard curves

Atkinson and Goda's 2010 interim updated seismic hazard model (AG10) provides the necessary data to conduct probabilistic seismic hazard analysis (PSHA) for both eastern and western Canada. It is an interim model since it merely focuses on key uncertainties in PSHA, which are seismicity rates and GMPEs. Similarly to Atkinson and Boore's 2006 model, these new equations take into account soil amplification factors to generate PSHA results for various soil conditions. Also, it is important to know that Atkinson and Goda's 2010 interim updated seismic hazard model should be viewed as a complementary to the existing GSC 1995 model that is the basis of the NBCC 2005 and 2010, and provides information on the updated regional seismicity rates and ground-motion models since 1995 (Carleton University, 2011). Figures 4.4 to 4.7 show Montreal and Vancouver's hazard curves for two site conditions (Vs30 = 555 and 200 m/s). In

other words, the average shear-wave velocity in the uppermost 30 m Vs30 is set to 555 and 200 (m/s). These correspond to NEHRP site class C and D respectively.

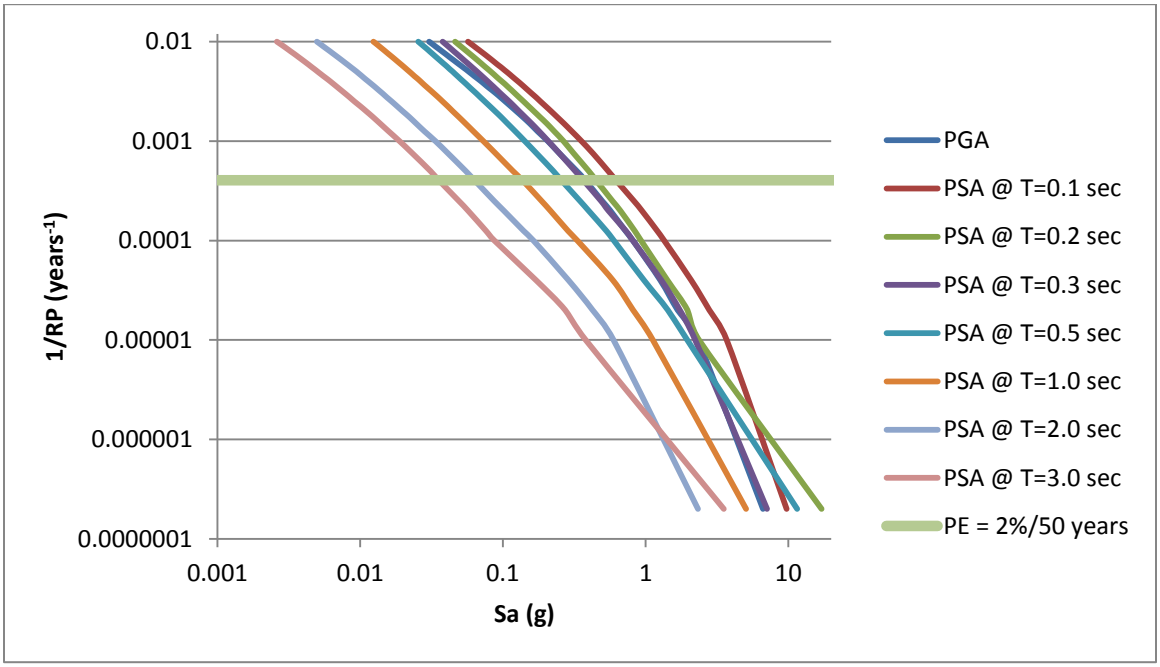

Figure 4.4: AG10 Montreal site class C hazard curves

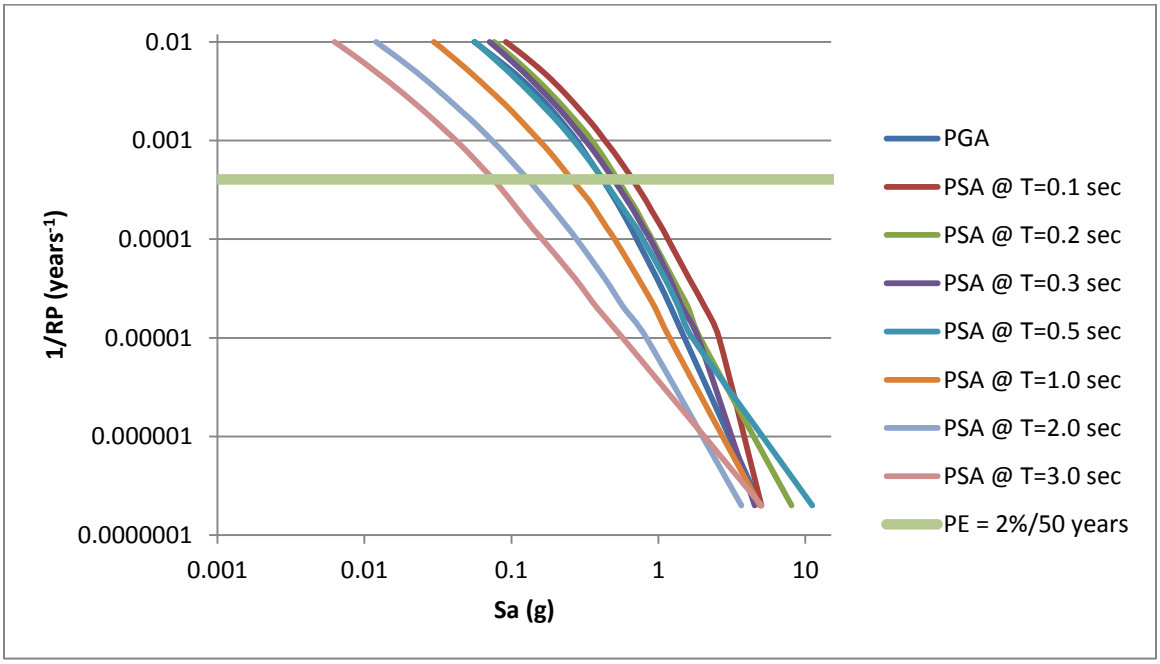

Figure 4.5: AG10 Montreal site class D hazard curves

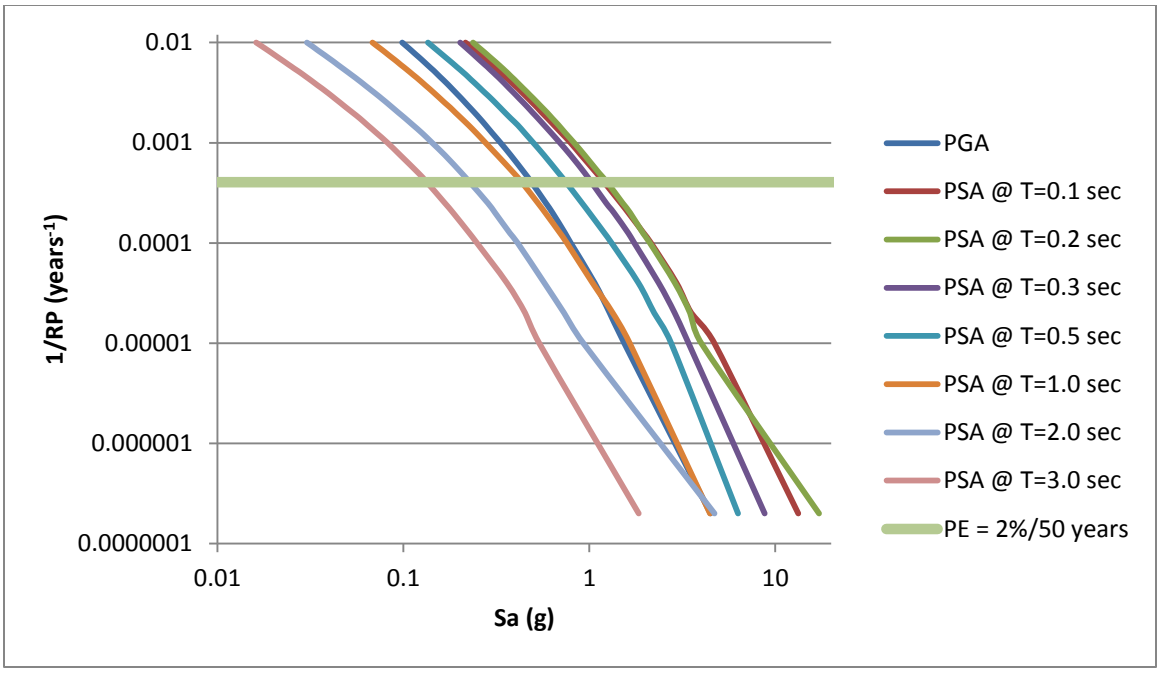

Figure 4.6: AG10 Vancouver site class C hazard curves

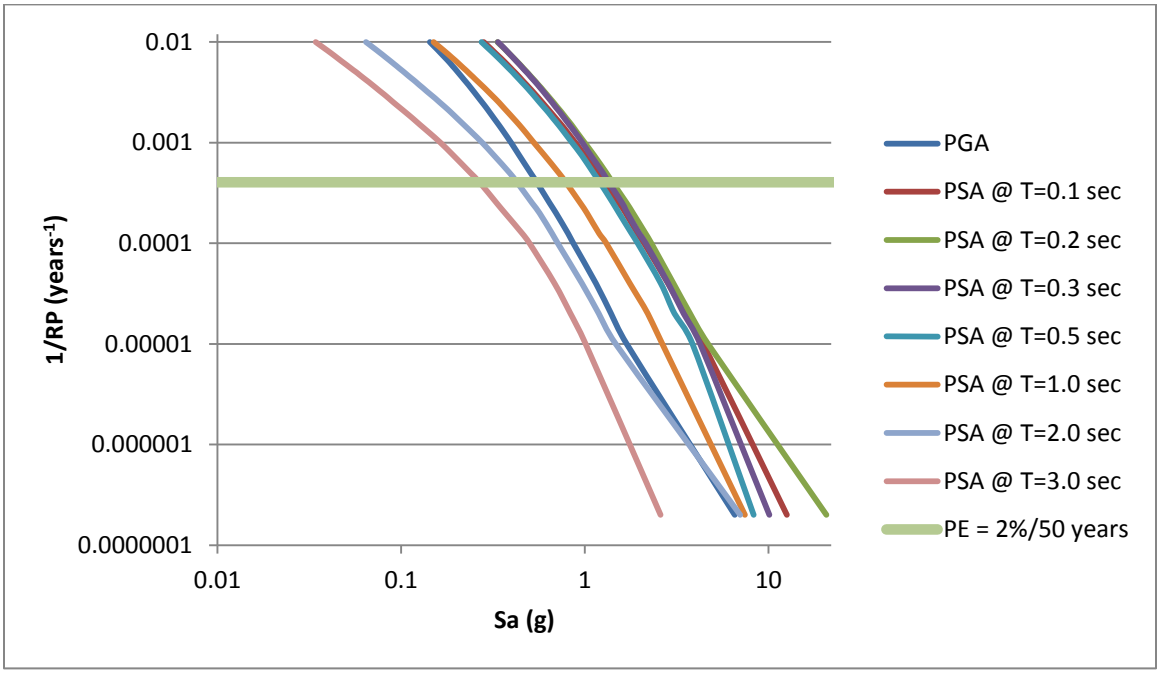

Figure 4.7: AG10 Vancouver site class D hazard curves

AG10 model's ground-motion parameter values are obtained from a Monte Carlo simulation for a period of five million years. Therefore, at a return period of 100,000

years, the results become considerably unreliable since only approximately 200 samples are available. Also, it is important to keep in mind that AG10 model is continuously being updated and results are expected to change slightly over the years.

4.2 Madrid Bridge Analysis

The Madrid Bridge is a regular four-span continuous bridge structure, shown in Figure 4.8, and is analyzed under thermal and seismic loading of the CHBDC CSA-S6-06.

Figure 4.8: Madrid Bridge (Guizani, 2007)

This 128.8 m long bridge has two expansion joints at both ends and a superstructure composed of four steel beams and a reinforced concrete deck. The

isolation bearings are designed to provide an equivalent viscous damping β of 17.7 % and a longitudinal period of seismically isolated structure T_e of 1.87 sec. Finally, the bridge is categorised as a lifeline bridge by the Quebec Ministry of Transportation (MTQ) and is located near Drummondville and Victoriaville on Highway 20 over the Nicolet River in the province of Quebec (Guizani, 2007). However, the bridge is analyzed for the purpose of this thesis using Montreal and Vancouver's climatic and seismic exposures.

4.2.1 Thermal Displacements of Madrid Bridge

To calculate the thermal displacements of the Madrid Bridge in Montreal and Vancouver, a site specific analysis was conducted using climatic data from the Montreal Pierre-Elliott Trudeau Airport and Vancouver International Airport (Environment Canada, 2011). Figures 4.9 and 4.10 illustrate the effective daily temperature at both locations from January 1st 1980 to December 31st 2010 by using the characteristics of the Madrid Bridge.

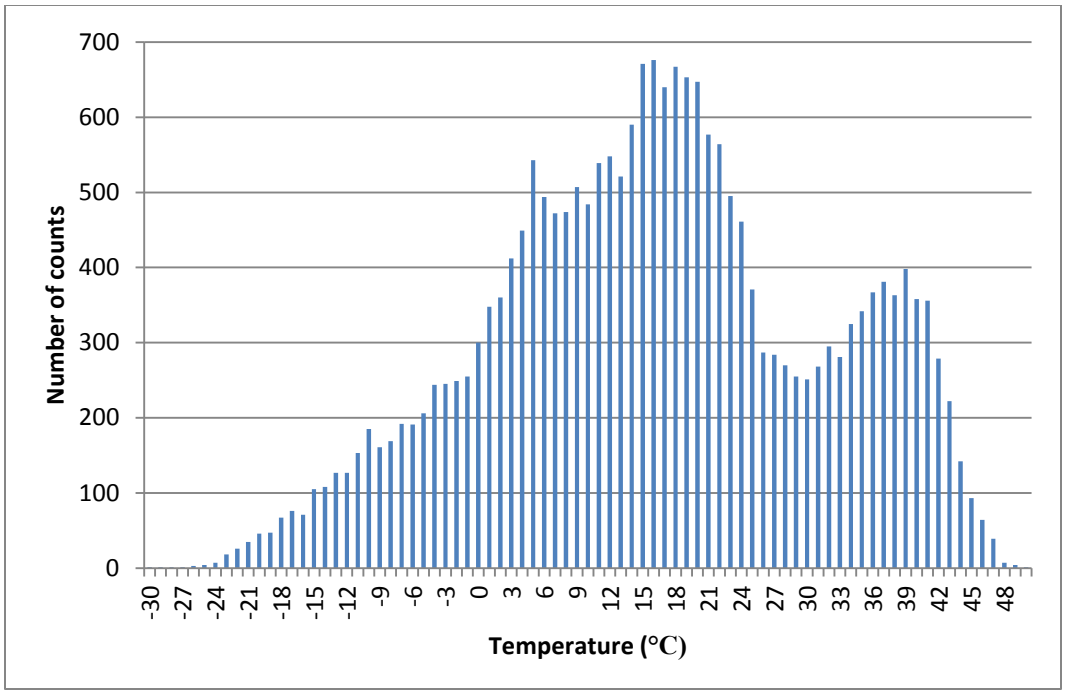

Figure 4.9: Effective daily temperature histogram from 1980-2010 for the Madrid Bridge (Montreal climate)

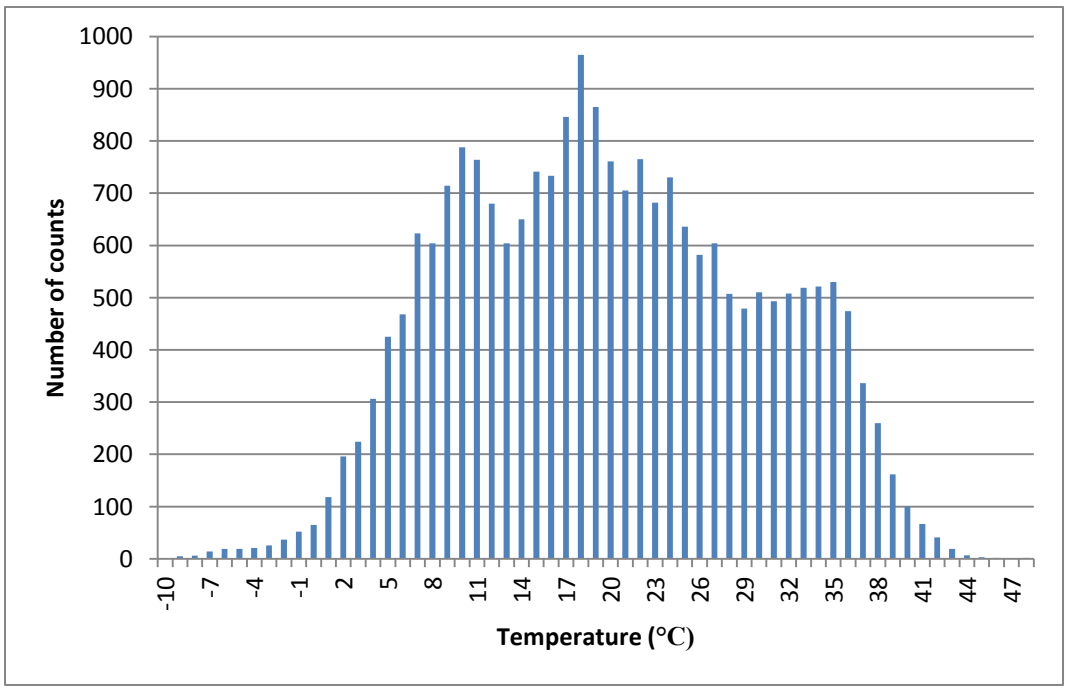

Figure 4.10: Effective daily temperature histogram from 1980-2010 for the Madrid Bridge (Vancouver climate)

The effective temperatures are a function of the materials of the bridge's superstructure. Since the superstructure of the Madrid Bridge falls in the CHBDC CSA-S6-06 Type B category and has a depth of 1.903 m, its effective daily temperature range varies from -30°C to 50°C in Montreal and from -10°C to 48°C in Vancouver (CSA, 2006a).

When the Madrid Bridge is subjected to the CHBDC CSA-S6-06 climatic chart instead of actual data, the effective daily temperature ranges for Montreal and Vancouver vary from -31.6°C to 41.4°C and -9.6°C to 39.4°C respectively.

Given the effective temperatures, the thermal displacements, $\Delta_{thermal}$, can be calculated as,

$$\Delta_{thermal} = \alpha \times L \times \Delta T_{max} \quad (4.1)$$

where

α = thermal coefficient of bridge superstructure = 11 x $10^{-6}/^{0}$C for steel beams with a concrete deck

L = length of the member subjected to deformation = 128.8/2 = 64.4 m = 64,400 mm

ΔT_{max} = maximum temperature differential after onsite installation, °C

The bridge is presumed to be installed at 15 ^{o}C. Therefore, the maximum temperature differentials and thermal displacements are shown in Table 4.1.

Table 4.1: Maximum thermal displacements of the Madrid Bridge

Climatic Database	**Location**	**ΔT_{max} (°C)**	**$\Delta_{thermal\ max}$ (mm)**
Environment Canada	Montreal	45.0	31.9
	Vancouver	33.0	23.4
CHBDC CSA-S6-06	Montreal	46.6	33.0
	Vancouver	24.6	17.4

When calculating design displacements of base isolators, it is not important whether the members are shrinking or elongating. What is important is the maximum displacement generated in one direction. Therefore, absolute thermal displacements, $|\Delta_{thermal}|$, are considered in the analyses of this thesis, since bridge isolators have the same capacity whether bridge members shrink or elongate (CSA, 2006b). Figures 4.11 and 4.12 present $|\Delta_{thermal}|$ values associated with Montreal and Vancouver`s climatic data from 1980 to 2010.

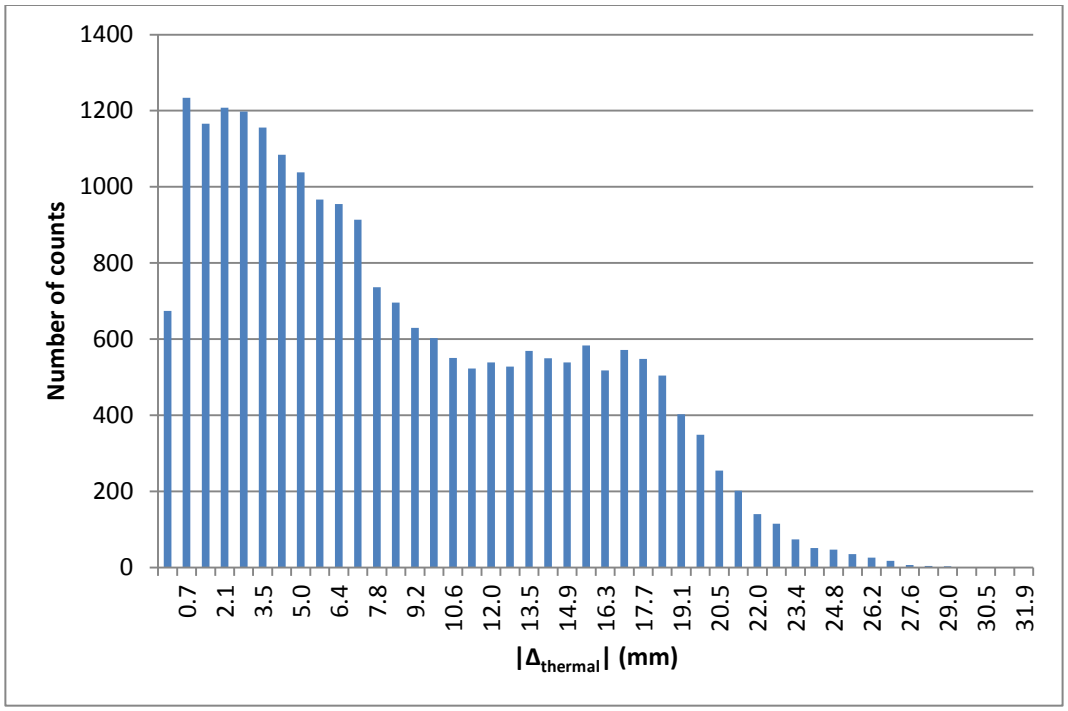

Figure 4.11: Histogram of $|\Delta_{thermal}|$ for the Madrid Bridge from 1980-2010 (Montreal climate)

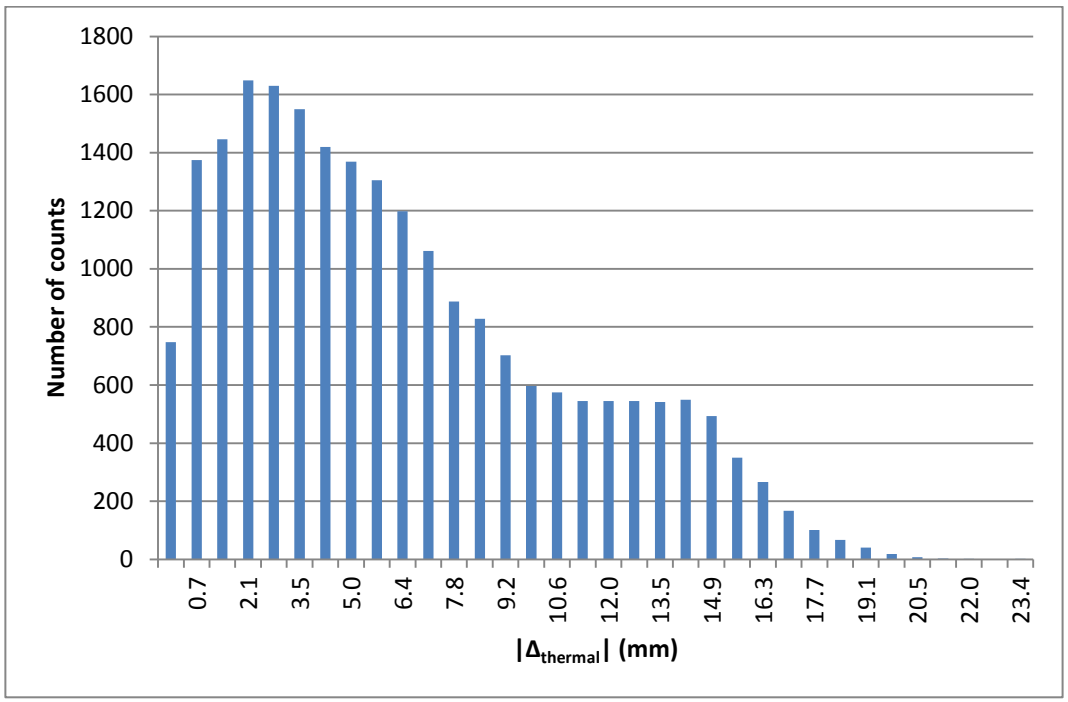

Figure 4.12: Histogram of $|\Delta_{thermal}|$ for the Madrid Bridge from 1980-2010 (Vancouver climate)

4.2.2 Seismic Displacements of Madrid Bridge

The longitudinal seismic displacements, $\Delta_{seismic}$, of the Madrid Bridge are calculated using the Atkinson and Boore 2006 (AB06) and Atkinson and Goda 2010 (AG10) new seismicity models and GMPEs. The displacements are determined by the uniform-load/single-mode spectral method of the CHBDC CSA-S6-06. As well, the UHS of AB06 and AG10 models are compared to the design response spectrum of the CHBDC CSA-S6-06 in Figure 4.13.

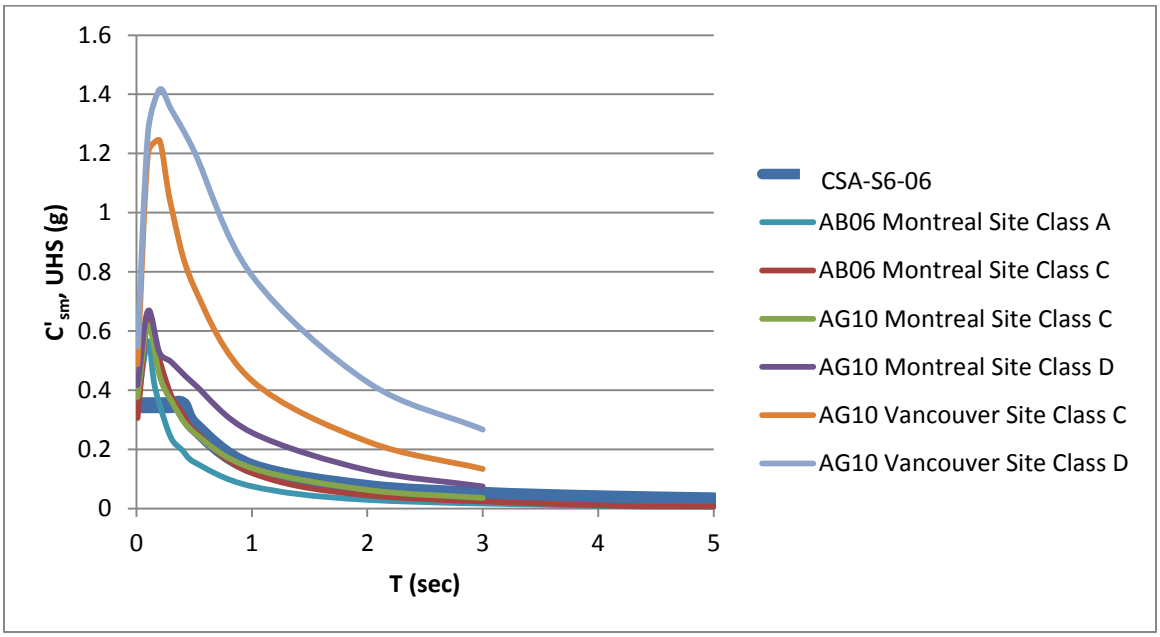

Figure 4.13: CSA-S6-06 response spectrum of Madrid Bridge and UHS of AB06 and AG10 models

The normalized elastic seismic response coefficient C'_{sm}, derived from the elastic response spectra, is directly related to the ground response spectra. C'_{sm} is specified in

terms of a design displacement d_i, which is a function of the zonal acceleration ratio A, the site coefficient S_i, the period of the seismically isolated structure T_e, and the coefficient, B, for effective damping of the isolated structure. According to the CHBDC CSA-S6-06, Montreal and Vancouver have the same C'sm parameters and therefore the design spectrum is identical in both locations. Also, a reference ground condition similar to NEHRP site class C is established in the CHBDC CSA-S6-06 to compare seismic hazard levels across Canada. Therefore, practically all the site class C UHS from Figure 4.13 are similar to the bridge's design spectrum. Note however that AG10 Vancouver site class C UHS is practically twice that of Montreal.

One the UHSs are calculated, the longitudinal spectral displacements can be determined by using equation 4.2 both for AB06 and AG10.

$$\Delta_{seismic} = S_D = (250 \times S_a \times S_i \times T^2)/B \qquad (4.2)$$

where

S_a = spectral acceleration, g

S_i = site coefficient

T = natural period of vibration, sec

B = effective damping coefficient of the isolation system

The seismic displacements are presented in Table 4.2, and graphically in Figure 4.14.

Table 4.2: Seismic displacements in mm of Madrid Bridge at 2%/50 years

Seismic Hazard Model	T=0.01 sec	T=0.1 sec	T=0.15 sec	T=0.2 sec	T=0.3 sec	T=0.4 sec	T=0.5 sec	T=1.0 sec	T=2.0 sec	T=3.0 sec	T=4.0 sec	T=5.0 sec	Te=1.87 sec
AB06 Montreal Site Class A	0.01	0.99	1.70	2.46	3.76	5.49	6.87	13.16	20.65	-	26.70	27.63	**19.68**
AB06 Montreal Site Class C	0.01	1.15	2.28	3.51	6.03	8.99	11.54	21.02	31.48	-	31.68	32.27	**30.12**
AG10 Montreal Site Class C	0.01	1.08	-	3.14	5.75	-	11.21	23.95	44.18	55.90	-	-	**41.55**
AG10 Montreal Site Class D	0.01	1.17	-	3.68	7.81	-	18.41	44.82	90.67	118.63	-	-	**84.71**
AG10 Vancouver Site Class C	0.01	2.10	-	8.70	16.11	-	32.71	75.56	158.84	210.10	-	-	**148.02**
AG10 Vancouver Site Class D	0.01	2.22	-	9.89	21.22	-	52.76	137.73	298.74	420.27	-	-	**277.81**

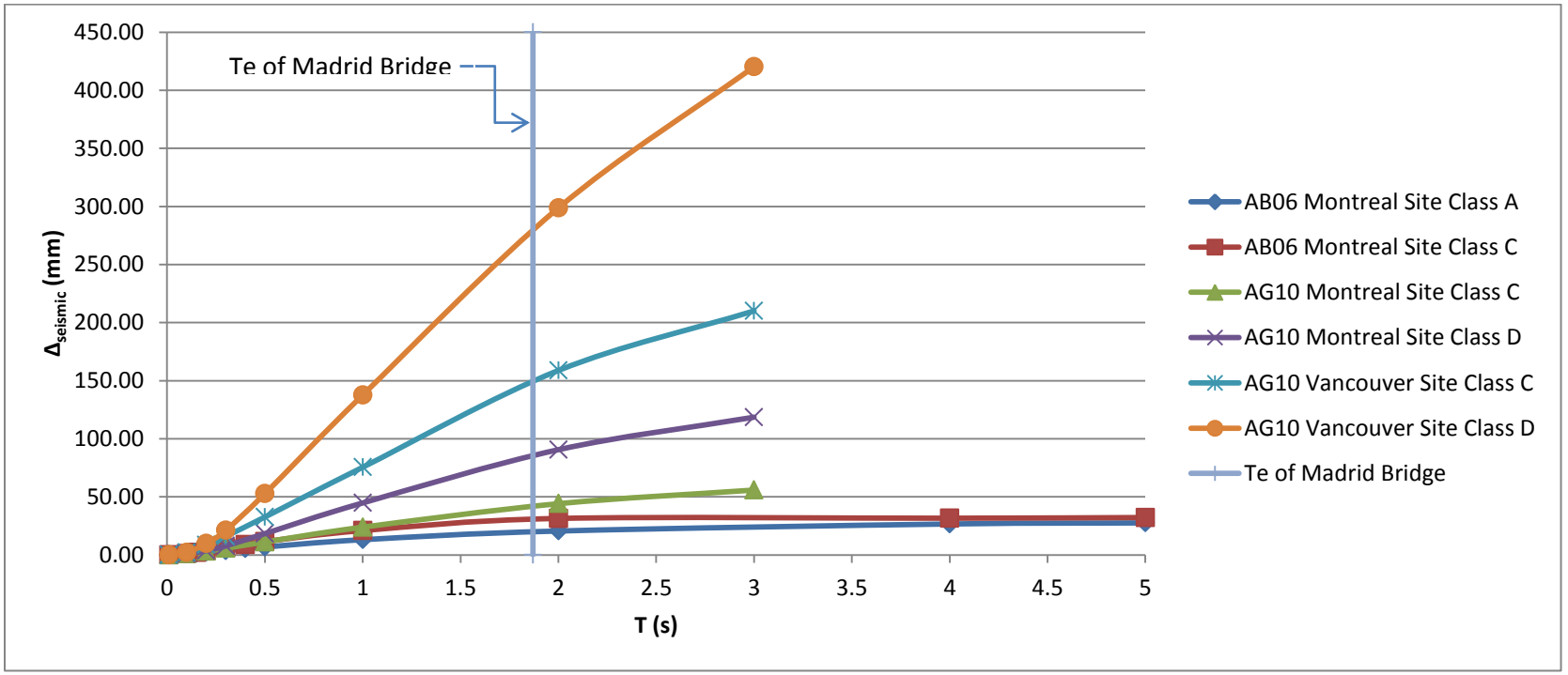

Figure 4.14: Seismic displacements of Madrid Bridge for different seismic hazard models

4.2.3 Combination of Thermal and Seismic Displacements of Madrid Bridge

To develop a combination equation for thermal and seismic displacements, the total probability theorem and Turkstra's rule are utilized. In this thesis, the Madrid Bridge and the A30 Bridge are analyzed with Montreal's climatic characteristics and seismic models, as well as for Vancouver's effective temperature readings and seismic zone. In other words, the bridge is analyzed as if it is located in Montreal or Vancouver. An example calculation is illustrated below for the two methods at a period of vibration of two seconds for the AG10 Montreal Site Class D UHS.

The first step in using the total probability theorem is to compute the seismic displacements as a function of probability of exceedance. A graphical illustration is presented in Figure 4.15.

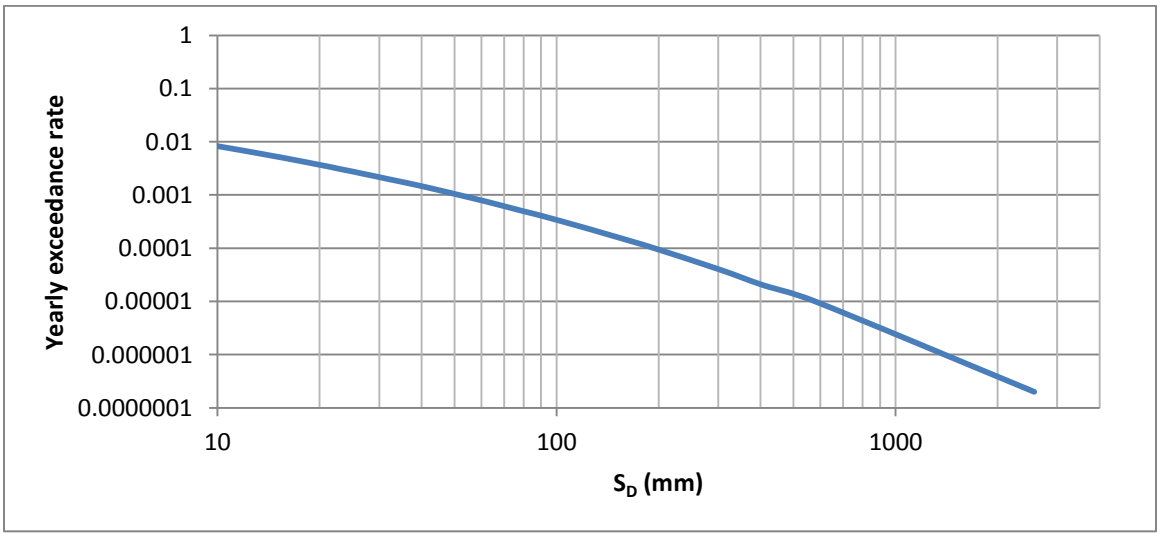

Figure 4.15: Spectral displacements as a function of yearly exceedance rate (AG10 Montreal site class D, T = 2 sec)

Then, using the effective daily temperature range applicable to the bridge, the thermal displacements for each temperature differential is combined with the spectral displacements. The maximum temperature differential for the Madrid Bridge in Montreal is equal to 45°C, since the effective temperature range is -30°C to 50°C, and the effective temperature at construction is assumed to be 15°C. Once all the displacements are calculated, the total probability theorem is applied as follows:

Step 1: Calculate the probability of occurrence, P_i, of each ΔT_i (see Table 4.3).

Step 2: Determine the seismic (spectral) displacement at a return period of 2475 years ($\Delta_{seismic}$ @ RP_1 = 2475 years).

Step 3: Linearly interpolate the values of each combined seismic and thermal displacement curve to find the associated $\lambda_i(\Delta T_i)$ value that generates the same displacement as $\Delta_{seismic}$ @ 2475 years.

Step 4: Calculate the sum of the product of $\lambda_i(\Delta T_i)$ and the probability of occurrence P_i of each thermal displacement found at step 1.

$\lambda_1 = \sum[P_i \times \lambda_i(\Delta T_i)] = 1/RP_{average\ 1}$

Step 5: Repeat steps 2, 3 and 4 for a new return period RP_2.

$\lambda_2 = \lambda(RP2) = \sum[P_i \times \lambda_i(\Delta T_i)] = 1/RP_{average\ 2}$

Stop if λ_2 is equal to 1/2475 otherwise modify RP and repeat. Once λ_N = 1/2475, the percentage of thermal displacement that should be combined with the maximum seismic displacement can be determined.

Table 4.3 illustrates how step 4 can generate a λ = 1/2475 with RP = 1/2858 or 0.000350 for the Madrid Bridge.

Table 4.3: Total probability theorem example for the Madrid Bridge (AG10 Montreal site class D, T = 2 sec)

ΔT_i	$\lambda(\Delta T_i)$	P_i	$\lambda(\Delta T_i)*P_i$		ΔT_i	$\lambda(\Delta T_i)$	P_i	$\lambda(\Delta T_i)*P_i$
0	0.000350	0.0299	1.04739E-05		23	0.000458	0.0230	1.05369E-05
1	0.000354	0.0548	1.93877E-05		24	0.000464	0.0254	1.1788E-05
2	0.000358	0.0518	1.85192E-05		25	0.000470	0.0243	1.14398E-05
3	0.000361	0.0537	1.93934E-05		26	0.000476	0.0224	1.06558E-05
4	0.000365	0.0532	1.94382E-05		27	0.000482	0.0179	8.62807E-06
5	0.000369	0.0513	1.89549E-05		28	0.000488	0.0155	7.56514E-06
6	0.000373	0.0481	1.79601E-05		29	0.000494	0.0113	5.59564E-06
7	0.000377	0.0461	1.73759E-05		30	0.000500	0.0090	4.48656E-06
8	0.000381	0.0429	1.63531E-05		31	0.000510	0.0062	3.17292E-06
9	0.000385	0.0424	1.63139E-05		32	0.000521	0.0051	2.6588E-06
10	0.000388	0.0406	1.57702E-05		33	0.000531	0.0033	1.74465E-06
11	0.000392	0.0327	1.28252E-05		34	0.000541	0.0023	1.22566E-06
12	0.000396	0.0309	1.22474E-05		35	0.000551	0.0021	1.15098E-06
13	0.000400	0.0280	1.1194E-05		36	0.000562	0.0016	8.73081E-07
14	0.000404	0.0268	1.08177E-05		37	0.000572	0.0012	6.60438E-07
15	0.000410	0.0245	1.0031E-05		38	0.000582	0.0008	4.65439E-07
16	0.000416	0.0232	9.66093E-06		39	0.000592	0.0003	1.84198E-07
17	0.000422	0.0239	1.01004E-05		40	0.000603	0.0002	1.07081E-07
18	0.000428	0.0234	1.00353E-05		41	0.000613	0.0001	8.16797E-08
19	0.000434	0.0253	1.09665E-05		42	0.000623	0.0000	2.76829E-08
20	0.000440	0.0244	1.07472E-05		43	0.000634	0.0000	2.81391E-08
21	0.000446	0.0239	1.06762E-05		44	0.000644	0.0000	2.85954E-08
22	0.000452	0.0259	1.17034E-05		45	0.000654	0.0000	2.90517E-08
					$1/RP_{average}$		1	**1/2475**

Once λ_2 is equal to 1/2475, the percentage of thermal displacement combined with the design seismic displacement may be determined with equation 4.3. Table 4.4 summarizes the percentage of thermal displacement for the case when the maximum effective temperature range is defined by Environment Canada's data and the CHBDC CSA-S6-06 specifications.

$$\Delta_{\text{thermal average}}/\Delta_{\text{thermal maximum}} = (\Delta_{\text{seismic @ }\lambda 2} - \Delta_{\text{seismic @ 1/2475}})/\Delta_{\text{thermal maximum}} = \%\Delta_{\text{thermal}} \quad (4.3)$$

Table 4.4: Total probability theorem results for Madrid Bridge AG10 Montreal site class D, T = 2 sec

Maximum effective temperature differential	**$\%\Delta_{\text{thermal}}$**
Environment Canada ($\Delta T_{\text{eff, max}} = 45^{o}C$)	31.2
CHBDC CSA-S6-06 ($\Delta T_{\text{eff, max}} = 47^{o}C$)	30.1

For the application of Turkstra's rule, only the spectral displacements with a return period of 2,475 and 247.5 years are needed for each period. As for thermal displacements, the average daily recorded displacement is required, as well as the maximum calculated displacements based on Environment Canada and the CHBDC CSA-S6-06 effective temperature range. Turkstra's rule is expressed as follows:

1) If Seismic Displacement Controls ($\Delta_{\text{seismic}} > \Delta_{\text{thermal}}$)

$$\Delta_{\text{seismic max}} + \Delta_{\text{thermal ave}} = \Delta_{\text{tot}} \quad (4.4)$$

$$\%\Delta_{\text{thermal}} = (\Delta_{\text{thermal ave}})/ (\Delta_{\text{thermal max Env. Canada}}) \quad (4.5)$$

$$\%\Delta_{thermal} = (\Delta_{thermal\ ave})/ (\Delta_{thermal\ max\ CSA\text{-}S6\text{-}06}) \quad (4.6)$$

2) If Thermal Displacement Controls ($\Delta_{thermal} > \Delta_{seismic}$)

$$\Delta_{thermal\ max} + \Delta_{seismic\ ave} = \Delta_{tot} \quad (4.7)$$

$$\%\Delta_{thermal} = ((\Delta_{thermal\ max\ Env.\ Canada} + \Delta_{seismic\ ave}) - \Delta_{seismic\ max})/(\Delta_{thermal\ max\ Env.\ Canada}) \quad (4.8)$$

$$\%\Delta_{thermal} = ((\Delta_{thermal\ max\ CSA\text{-}S6\text{-}06} + \Delta_{seismic\ ave}) - \Delta_{seismic\ max})/(\Delta_{thermal\ max\ CSA\text{-}S6\text{-}06}) \quad (4.9)$$

$$(\Delta_{thermal\ max} + \Delta_{seismic\ ave}) > \Delta_{seismic\ max} \text{ or else } \%\Delta_{thermal} = 0\% \quad (4.10)$$

The largest $\%\Delta_{thermal}$ from (1) or (2) is selected to represent the maximum value for the combined displacements.

For example, considering T = 2 sec and with the AG10 Montreal Site Class D spectra, Turkstra's rule is as follows:

1) If Seismic Displacement Controls ($\Delta_{seismic} > \Delta_{thermal}$)

$$\Delta_{seismic\ max} + \Delta_{thermal\ ave} = \Delta_{tot}$$

$$\%\Delta_{thermal} = (\Delta_{thermal\ ave})/ (\Delta_{thermal\ max\ Env.\ Canada}) = (8.7 \text{ mm} / 31.9 \text{ mm}) = 27.3\ \%$$

$$\%\Delta_{thermal} = (\Delta_{thermal\ ave})/ (\Delta_{thermal\ max\ CSA\text{-}S6\text{-}06}) = (8.7 \text{ mm} / 33.0 \text{ mm}) = 26.4\ \%$$

2) If Thermal Displacement Controls ($\Delta_{thermal} > \Delta_{seismic}$)

$$\Delta_{thermal\ max} + \Delta_{seismic\ ave} = \Delta_{tot} = \Delta_{seismic\ max} + \Delta_{thermal\ ave}$$

$$\%\Delta_{thermal} = ((\Delta_{thermal\ max\ Env.\ Canada} + \Delta_{seismic\ ave}) - \Delta_{seismic\ max})/(\Delta_{thermal\ max\ Env.\ Canada})$$

$$\%\Delta_{thermal} = (((31.9 \text{ mm} + 8.7 \text{ mm}) - 90.7 \text{ mm})/31.9 \text{ mm}) \times 100\ \% = -157\ \% = 0\ \%$$

$$\%\Delta_{thermal} = ((\Delta_{thermal\ max\ CSA\text{-}S6\text{-}06} + \Delta_{seismic\ ave}) - \Delta_{seismic\ max})/(\Delta_{thermal\ max\ CSA\text{-}S6\text{-}06})$$

$$\%\Delta_{thermal} = (((33.0 \text{ mm} + 8.7 \text{ mm}) - 90.7 \text{ mm})/33.0 \text{ mm}) \times 100\ \% = -148\ \% = 0\ \%$$

Table 4.5 summarizes Turkstra's rule using Environment Canada and the CHBDC CSA-S6-06 maximum thermal displacements.

Table 4.5: Turkstra's rule for Madrid Bridge (AG10 Montreal site class D, T = 2 sec)

Maximum effective temperature differential	**$\%\Delta_{thermal}$**
Environment Canada ($\Delta T_{eff,\,max} = 45^{o}C$)	27.3
CHBDC CSA-S6-06 ($\Delta T_{eff,\,max} = 47^{o}C$)	26.4

Since the period of the isolated Madrid Bridge is 1.87 sec, only periods of vibration of 0.5 sec and up are relevant for the analysis. Table 4.6 summarizes the percentage of thermal displacements to combine with the design seismic displacement for both load combination methods.

The importance factor of the bridge is also considered in the analysis. Based on the Eurocode 8 method of analysis, all seismic displacements are multiplied by a factor of 1.5 to increase the design displacements of lifeline bridges and modify $\%\Delta_{thermal}$. Table 4.7 illustrates the new $\%\Delta_{thermal}$ values which take into account the importance factor of the Madrid Bridge.

Table 4.6: $\%\Delta_{thermal}$ to combine with $\Delta_{seismic}$ for all seismic hazard models and both load combination methods for the Madrid Bridge

Seismic Hazard Model	Load Combination Method	Climatic Database	T=0.5 sec	T=1.0 sec	T=2.0 sec	T=3.0 sec	T=4.0 sec	T=5.0 sec	Te=1.87 sec
AB06 Montreal Site Class A	Total Probability Theorem	Env. Canada	53.0	45.5	38.2	-	34.7	33.8	**39.2**
		CSA-S6-06	51.2	43.9	36.9	-	33.5	32.6	**37.8**
	Turkstra's Rule	Env. Canada	84.3	70.2	52.6	-	34.4	31.1	**54.9**
		CSA-S6-06	84.8	71.3	54.3	-	36.6	33.4	**56.5**
AB06 Montreal Site Class C	Total Probability Theorem	Env. Canada	49.2	37.6	33.8	-	33.3	32.7	**34.3**
		CSA-S6-06	47.5	36.3	32.6	-	32.2	31.5	**33.1**
	Turkstra's Rule	Env. Canada	73.6	52.3	27.6	-	27.2	27.2	**30.8**
		CSA-S6-06	74.5	53.9	30.1	-	26.5	26.2	**33.2**
AG10 Montreal Site Class C	Total Probability Theorem	Env. Canada	42.7	35.1	33.3	33.4	-	-	**33.6**
		CSA-S6-06	41.3	33.9	32.2	32.2	-	-	**32.4**
	Turkstra's Rule	Env. Canada	72.0	39.3	27.2	27.2	-	-	**28.7**
		CSA-S6-06	73.0	41.3	26.2	26.2	-	-	**28.2**
AG10 Montreal Site Class D	Total Probability Theorem	Env. Canada	38.9	33.9	31.2	30.6	-	-	**31.5**
		CSA-S6-06	37.6	32.7	30.1	29.5	-	-	**30.4**
	Turkstra's Rule	Env. Canada	57.4	27.2	27.2	27.2	-	-	**27.2**
		CSA-S6-06	58.9	26.2	26.2	26.2	-	-	**26.2**
AG10 Vancouver Site Class C	Total Probability Theorem	Env. Canada	33.1	30.8	31.2	31.0	-	-	**31.2**
		CSA-S6-06	44.3	41.3	41.9	41.5	-	-	**41.8**
	Turkstra's Rule	Env. Canada	27.0	27.0	27.0	27.0	-	-	**27.0**
		CSA-S6-06	36.2	36.2	36.2	36.2	-	-	**36.2**
AG10 Vancouver Site Class D	Total Probability Theorem	Env. Canada	32.0	30.6	30.6	30.0	-	-	**30.6**
		CSA-S6-06	42.9	41.1	41.1	40.2	-	-	**41.1**
	Turkstra's Rule	Env. Canada	27.0	27.0	27.0	27.0	-	-	**27.0**
		CSA-S6-06	36.2	36.2	36.2	36.2	-	-	**36.2**

Table 4.7: $\%\Delta_{thermal}$ to combine with $\Delta_{seismic}$ when importance factor is taken into consideration for the Madrid Bridge

Seismic Hazard Model	Load Combination Method	Climatic Database	T=0.5 sec	T=1.0 sec	T=2.0 sec	T=3.0 sec	T=4.0 sec	T=5.0 sec	Te=1.87 sec
I = 1.5 AB06 Montreal Site Class A	Total Probability Theorem	Env. Canada	49.4	39.2	34.1	-	32.1	31.8	**34.8**
		CSA-S6-06	47.7	37.8	32.9	-	31.0	30.7	**33.6**
	Turkstra's Rule	Env. Canada	76.4	55.4	29.0	-	27.2	27.2	**32.4**
		CSA-S6-06	77.2	71.3	31.4	-	26.2	26.2	**36.6**
I = 1.5 AB06 Montreal Site Class C	Total Probability Theorem	Env. Canada	40.5	33.1	30.8	-	32.2	30.7	**31.1**
		CSA-S6-06	39.1	32.0	29.8	-	31.0	29.6	**30.1**
	Turkstra's Rule	Env. Canada	60.5	28.4	27.2	-	27.2	27.2	**27.3**
		CSA-S6-06	61.8	30.9	26.2	-	26.2	26.2	**26.8**
I = 1.5 AG10 Montreal Site Class C	Total Probability Theorem	Env. Canada	39.5	33.2	30.3	29.1	-	-	**30.7**
		CSA-S6-06	38.2	32.1	29.3	28.1	-	-	**29.6**
	Turkstra's Rule	Env. Canada	58.0	27.2	27.2	27.2	-	-	**27.2**
		CSA-S6-06	59.4	26.2	26.2	26.2	-	-	**26.2**
I = 1.5 AG10 Montreal Site Class D	Total Probability Theorem	Env. Canada	34.7	30.2	30.7	29.5	-	-	**30.6**
		CSA-S6-06	33.5	29.2	29.6	28.5	-	-	**29.6**
	Turkstra's Rule	Env. Canada	36.1	27.2	27.2	27.2	-	-	**27.2**
		CSA-S6-06	38.3	26.2	26.2	26.2	-	-	**26.2**
I = 1.5 AG10 Vancouver Site Class C	Total Probability Theorem	Env. Canada	29.0	27.2	27.2	27.2	-	-	**27.2**
		CSA-S6-06	38.9	36.5	36.5	36.5	-	-	**36.5**
	Turkstra's Rule	Env. Canada	27.0	27.0	27.0	27.0	-	-	**27.0**
		CSA-S6-06	36.2	36.2	36.2	36.2	-	-	**36.2**
I = 1.5 AG10 Vancouver Site Class D	Total Probability Theorem	Env. Canada	31.0	28.9	27.2	27.1	-	-	**27.4**
		CSA-S6-06	41.6	38.7	36.5	36.3	-	-	**36.8**
	Turkstra's Rule	Env. Canada	27.0	27.0	27.0	27.0	-	-	**27.0**
		CSA-S6-06	36.2	36.2	36.2	36.2	-	-	**36.2**

Temperature can also affect the performance characteristics of the base isolation bearings. More specifically, the stiffness K, damping β, and energy dissipation per cycle (EDC) are altered by temperature variations (HITEC, 1998a & 1998b). Temperature effects on LRBs are summarized in Table 4.8, and on FPI bearings in Table 4.9.

Table 4.8: Dynamic performance characteristics of LRBs at temperature extremes (HITEC, 1998a)

Performance Parameters	**Cold Temperature 49 hrs @ -20°F**	**Ambient Temperature 70°F**	**Hot Temperature 23 hrs @ 120°F**
Stiffness (kips/in)	17.0 (+56 %)	10.9	10.4 (-5 %)
Damping (% Critical)	36.7 (-3 %)	37.8	35.1 (-7 %)
EDC (in-kips)	2900.0 (+45 %)	2004.0	1777.0 (-11 %)

Table 4.9: Dynamic performance characteristics of FPI Bearings at temperature extremes (HITEC, 1998b)

Performance Parameters	**Cold Temperature 49 hrs @ -40°F**	**Ambient Temperature 70°F**	**Hot Temperature 23 hrs @ 120°F**
Stiffness (kips/in)	7.9 (+0 %)	7.8	7.1 (-9 %)
Damping (% Critical)	23.9 (-6 %)	25.5	22.9 (-10 %)
EDC (in-kips)	1044.0 (+8 %)	968.8	917.0 (-5 %)

Dynamic properties of bearings have an impact on the seismic design displacements. However, thermal displacements are based on material properties that

remain practically constant as a function of temperature. Therefore, the thermal and seismic displacement combination demand must account for this effect.

To calculate the temperature adjusted seismic displacements, the longitudinal period of the seismically isolated structure, T_e, and the equivalent viscous damping, β, must be determined based on the data of Table 4.8 and Table 4.9. The ambient temperature of the Madrid Bridge is set to 15 ^{0}C with T_e equal to 1.87 sec and β to 17.7 % for the purpose of the adjustments.

The following details the calculation of LRBs:

At -28.9 ^{0}C (-20 ^{0}F), K increases by 56 %. And by using equation 1.2,

$$T = 2\pi\sqrt{\frac{M}{K}} \tag{1.2}$$

$$T \text{ @ } -28.9\ ^0\text{C} = 1.50 < 1.87 \text{ sec}$$

Also, at -28.9 ^{0}C (-20 ^{0}F), β decreases by 3 %.

$$\beta \text{ @ } -28.9\ ^0\text{C} = 17.7\ \% \times 0.97 = 17.17\ \%$$

Therefore, from Table 4.8 of CHBDC CSA-S6-06, B @ 17.17 % = 1.415

On the other hand, at 48.9 ^{0}C (120 ^{0}F), K decreases by 5 %. Thus by using equation 1.2,

$$T \text{ @ } 48.9\ ^0\text{C} = 1.92 > 1.87 \text{ sec}$$

And, at 48.9 ^{0}C (120 ^{0}F), β decreases by 7 %.

$$\beta \text{ @ } 48.9\ ^0\text{C} = 17.7\ \% \times 0.93 = 16.46\ \%$$

So, from Table 4.8 of CHBDC CSA-S6-06, B @ 16.46 % = 1.394

As for the calculations of FPI bearings:

At -40 ^{0}C (-40 ^{0}F), K does not change. Therefore,

$$T \text{ @ } -40\ ^0\text{C} = 1.87 = 1.87 \text{ sec}$$

Also at -40 ^{0}C (-40 ^{0}F), β decreases by 6 %.

$$\beta \text{ @ } -40\ ^0\text{C} = 17.7\ \% \times 0.94 = 16.64\ \%$$

Therefore, from Table 4.8 of the CHBDC CSA-S6-06, B @ 16.64 % = 1.399

At 48.9 ^{0}C (120 ^{0}F), K decreases by 9 %. Consequently, by using equations 1.3 and 1.4,

$$K = \frac{W}{R} \tag{1.3}$$

$$T = 2\pi\sqrt{\frac{R}{g}} \tag{1.4}$$

$$T \text{ @ } 48.9\ ^0\text{C} = 1.96 > 1.87 \text{ sec}$$

And at 48.9 ^{0}C (120 ^{0}F), β decreases by 10 %.

$$\beta \text{ @ } 48.9\ ^0\text{C} = 17.7\ \% \times 0.90 = 15.93\ \%$$

Thus, from Table 4.8 of CHBDC CSA-S6-06, B @ 15.93 % = 1.378

Finally, the values of T_e and B are illustrated graphically in Figures 4.16 and 4.17 as a function of temperature.

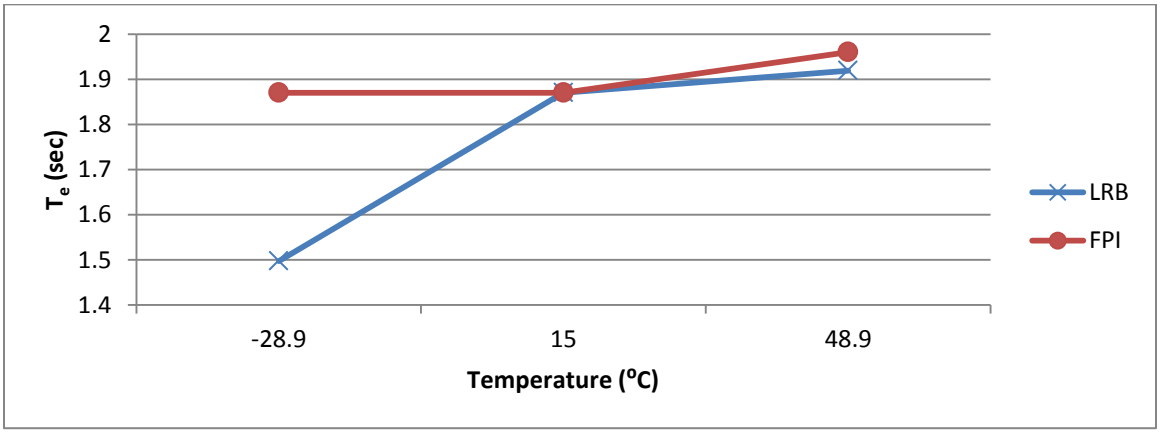

Figure 4.16: T_e values for Madrid Bridge as a function of temperature

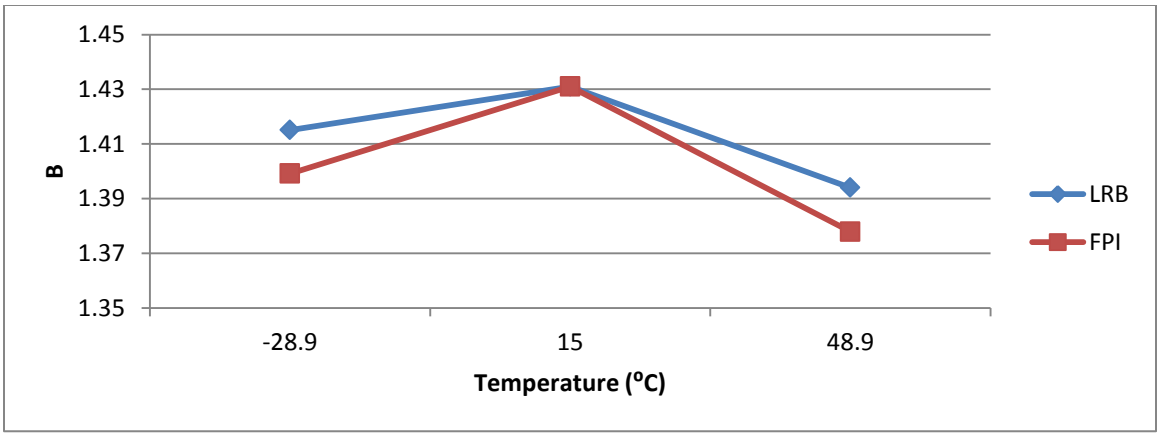

Figure 4.17: B values for Madrid Bridge as function of temperature

The thermal and seismic combination displacement demand formula, which takes into account the performance characteristics of the isolation bearings, is developed in this thesis with the total probability theorem. Turkstra's rule is not applicable since it does not take into consideration seismic displacements other than at ambient temperature. For this application, the thermal displacements are combined with the seismic displacements for each incremental temperature differential, instead of absolute temperature differentials. Table 4.10 summarizes the results when the performance characteristics of the bearings are taken into consideration.

Table 4.10: $\%\Delta_{thermal}$ to combine with $\Delta_{seismic}$ when performance characteristics and importance factor are taken into consideration for the Madrid Bridge

Seismic Hazard Model	Bearing Type	Climatic Data	T=0.5 sec	T=1.0 sec	T=2.0 sec	T=3.0 sec	T=4.0 sec	T=5.0 sec	Te=1.87 sec
AB06 Montreal Site Class A	LRB	Env. Canada	53.0	45.7	38.7	-	35.4	34.5	**39.6**
		CSA-S6-06	51.2	44.1	37.4	-	34.1	33.3	**38.3**
	FPI	Env. Canada	53.1	45.8	39.0	-	35.7	34.8	**39.9**
		CSA-S6-06	51.2	44.2	37.6	-	34.5	33.6	**38.5**
I=1.5 AB06 Montreal Site Class A	LRB	Env. Canada	51.1	39.5	34.9	-	33.1	32.8	**35.5**
		CSA-S6-06	49.4	38.2	33.7	-	31.9	31.6	**34.3**
	FPI	Env. Canada	51.1	39.7	35.3	-	33.6	33.3	**35.9**
		CSA-S6-06	49.4	38.4	34.1	-	32.4	32.1	**34.6**
AB06 Montreal Site Class C	LRB	Env. Canada	49.3	38.1	34.6	-	34.1	33.4	**35.1**
		CSA-S6-06	47.6	36.8	33.4	-	33.0	32.3	**33.9**
	FPI	Env. Canada	49.3	38.4	35.0	-	34.5	33.8	**35.4**
		CSA-S6-06	47.6	37.1	33.8	-	33.3	32.7	**34.2**
I=1.5 AB06 Montreal Site Class C	LRB	Env. Canada	40.8	33.9	32.0	-	33.3	31.8	**32.2**
		CSA-S6-06	39.4	32.8	30.9	-	32.1	30.7	**31.1**
	FPI	Env. Canada	40.9	34.3	32.5	-	33.9	32.4	**32.8**
		CSA-S6-06	39.5	33.1	31.4	-	32.7	31.3	**31.7**
AG10 Montreal Site Class C	LRB	Env. Canada	42.9	35.7	34.4	34.8	-	-	**34.6**
		CSA-S6-06	41.5	34.5	33.2	33.6	-	-	**33.4**
	FPI	Env. Canada	43.0	36.0	35.0	35.5	-	-	**35.1**
		CSA-S6-06	41.6	34.8	33.8	34.3	-	-	**33.9**
I=1.5 AG10 Montreal Site Class C	LRB	Env. Canada	40.1	34.1	32.0	31.1	-	-	**32.3**
		CSA-S6-06	38.7	32.9	30.9	30.1	-	-	**31.2**
	FPI	Env. Canada	40.2	34.5	32.9	32.2	-	-	**33.1**
		CSA-S6-06	38.9	33.3	31.8	31.1	-	-	**32.0**
AG10 Montreal Site Class D	LRB	Env. Canada	39.5	35.0	33.3	33.2	-	-	**33.5**
		CSA-S6-06	38.1	33.8	32.1	32.1	-	-	**32.3**
	FPI	Env. Canada	39.7	35.6	34.4	34.6	-	-	**34.5**
		CSA-S6-06	38.3	34.4	33.2	33.5	-	-	**33.3**
I=1.5 AG10 Montreal Site Class D	LRB	Env. Canada	35.5	31.8	33.9	33.7	-	-	**33.7**
		CSA-S6-06	34.2	30.7	32.8	32.6	-	-	**32.5**
	FPI	Env. Canada	35.8	32.6	35.6	35.9	-	-	**35.2**
		CSA-S6-06	34.6	31.5	34.4	34.7	-	-	**34.0**
AG10 Vancouver Site Class C	LRB	Env. Canada	34.0	32.8	35.7	36.7	-	-	**35.3**
		CSA-S6-06	45.6	44.1	47.9	49.2	-	-	**47.4**
	FPI	Env. Canada	34.5	33.9	38.0	39.8	-	-	**37.5**
		CSA-S6-06	46.3	45.5	51.0	53.4	-	-	**50.3**
I=1.5 AG10 Vancouver Site Class C	LRB	Env. Canada	30.3	29.8	32.9	34.7	-	-	**32.5**
		CSA-S6-06	40.7	39.9	44.1	46.6	-	-	**43.5**
	FPI	Env. Canada	31.0	31.2	35.8	38.7	-	-	**35.2**
		CSA-S6-06	41.6	41.8	48.1	52.0	-	-	**47.3**
AG10 Vancouver Site Class D	LRB	Env. Canada	33.4	34.3	38.9	41.7	-	-	**38.3**
		CSA-S6-06	44.8	46.1	52.2	55.9	-	-	**51.4**
	FPI	Env. Canada	34.2	36.3	43.2	47.6	-	-	**42.3**
		CSA-S6-06	45.9	48.7	58.0	63.9	-	-	**56.8**
I=1.5 AG10 Vancouver Site Class D	LRB	Env. Canada	33.3	34.7	38.1	42.4	-	-	**37.6**
		CSA-S6-06	44.7	46.6	51.1	56.9	-	-	**50.5**
	FPI	Env. Canada	34.5	37.8	43.8	50.6	-	-	**43.0**
		CSA-S6-06	46.3	50.8	58.7	67.9	-	-	**57.7**

4.3 A30 Bridge Analysis

The A30 Bridge over the St-Lawrence River in Montreal, shown in Figure 4.18, is currently being built. It is a 1.89 km long concrete structure with a concrete deck.

Figure 4.18: A30 Bridge over the St-Lawrence River (ARUP, 2011)

More specifically, the structure consists of five precast, prestressed New England Bulb Tee (NEBT) girders, 2 m deep, with a 200 mm thick cast-in-place reinforced concrete deck. The A30 Bridge over the St-Lawrence River is similar to the Madrid Bridge, since it consists of twin structures, carrying two lanes per direction and is also classified as a lifeline bridge. The A30 Bridge has 42 spans of typically 45 m in length each and nine expansion joints. It has six-span continuous segments at both ends and six five-span continuous segments in between. Finally, the isolation bearings are designed to

provide an equivalent viscous damping β of 24 % and a longitudinal period of seismically isolated structure T_e of 2.2 sec (ARUP, 2011).

4.3.1 Thermal Displacements of A30 Bridge

Data from the Montreal's Pierre-Elliot Trudeau Airport and Vancouver International Airport are again selected to calculate the thermal displacements of the A30 Bridge over the St-Lawrence River to analyze the combination rules as a function of the climatic zones. The A30 Bridge has a different effective temperature range than the Madrid Bridge, since its superstructure is different. Figures 4.19 and 4.20 show the site specific effective daily temperature readings of the A30 Bridge from January 1st 1980 to December 31st 2010 according to Environment Canada's daily climate database (Environment Canada, 2011).

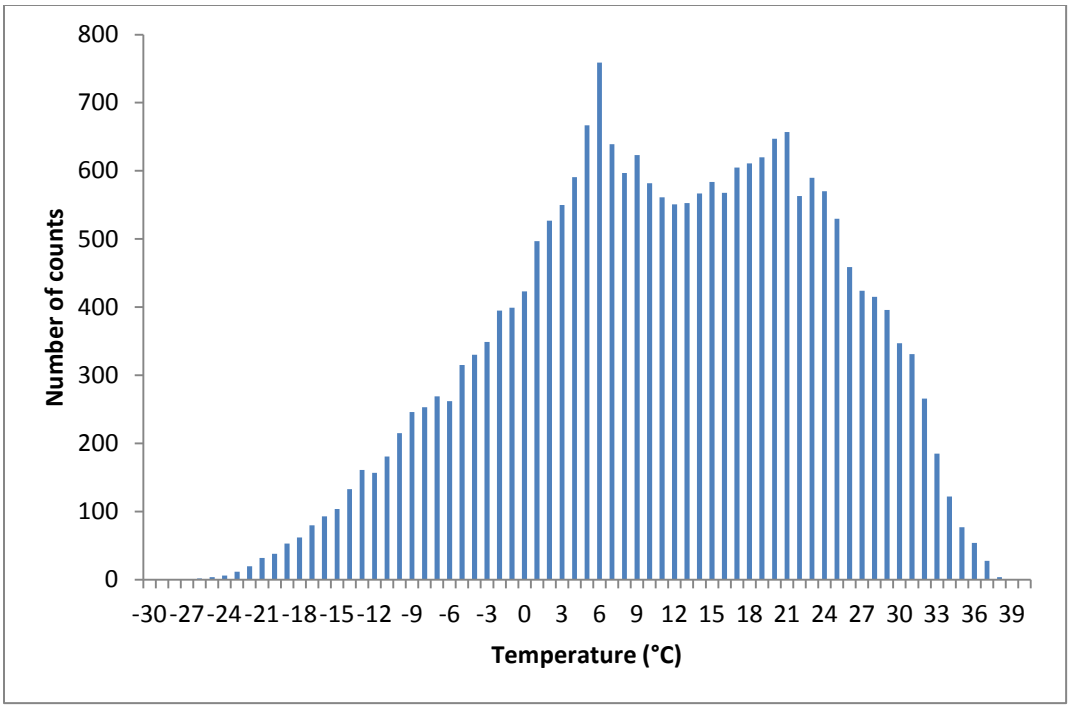

Figure 4.19: Effective daily temperature histogram from 1980-2010 for the A30 Bridge (Montreal climate)

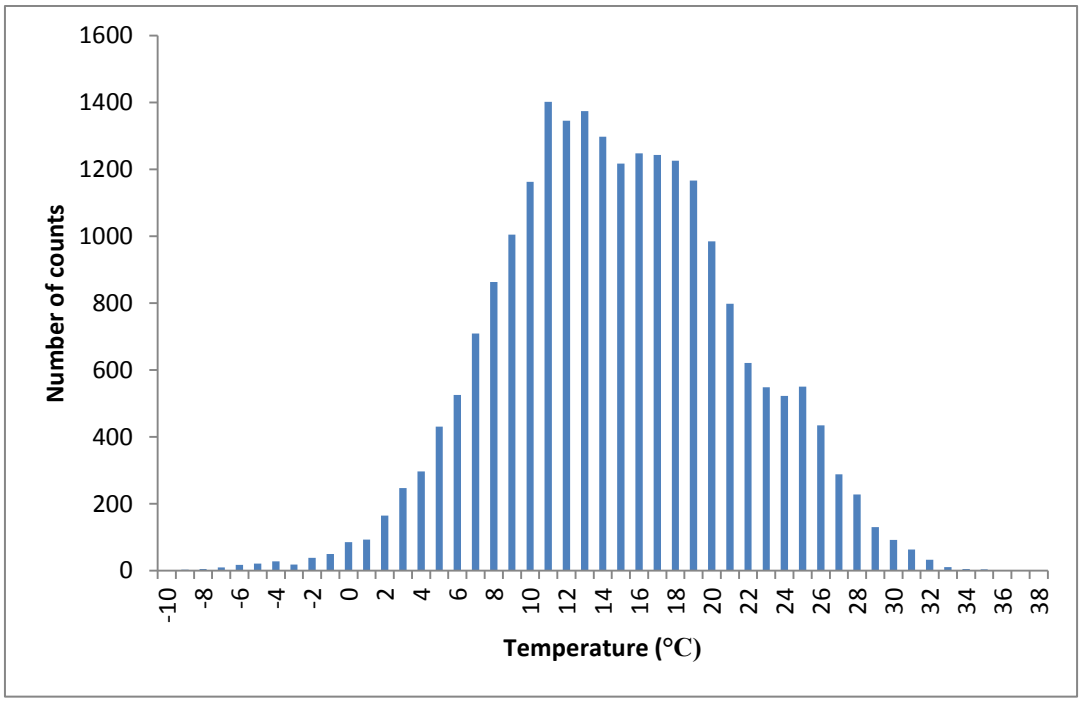

Figure 4.20: Effective daily temperature histogram from 1980-2010 for the A30 Bridge (Vancouver climate)

The superstructure of the A30 Bridge is categorised as a Type C superstructure in the CHBDC CSA-S6-06, and has a depth larger than 2 m. Therefore, based on Environment Canada climatic database, its effective daily temperature ranges from -30.0^{0}C to 40.0^{0}C in Montreal and from -10.0^{0}C to 38.0^{0}C in Vancouver. On the other hand, according to the Canadian Code's climatic database, Montreal's effective temperature range varies from -31.0°C to 31.0°C and Vancouver's effective temperature range varies from -9.0°C to 29.0°C for the A30 Bridge.

When using equation 4.1, α of the A30 Bridge is equal to 10 x $10^{-6}/^0$C because reinforced concrete girders with concrete deck are used, and L is equal to 135 m, since a six-span continuous segment was chosen for the analysis. The maximum temperature differentials and thermal displacements are shown in Table 4.11 for an effective construction temperature of 15^{o}C.

Table 4.11: Maximum thermal displacements of the A30 Bridge

Climatic Database	**Location**	**ΔT_{max} (°C)**	**$\Delta_{thermal\ max}$ (mm)**
Environment Canada	Montreal	45.0	60.8
	Vancouver	25.0	33.8
CHBDC CSA-S6-06	Montreal	46.0	62.1
	Vancouver	24.0	32.4

Figures 4.21 and 4.22 show histograms of absolute thermal displacements, $|\Delta_{thermal}|$, for the A30 Bridge from 1980-2010 for the Montreal and Vancouver climatic zones.

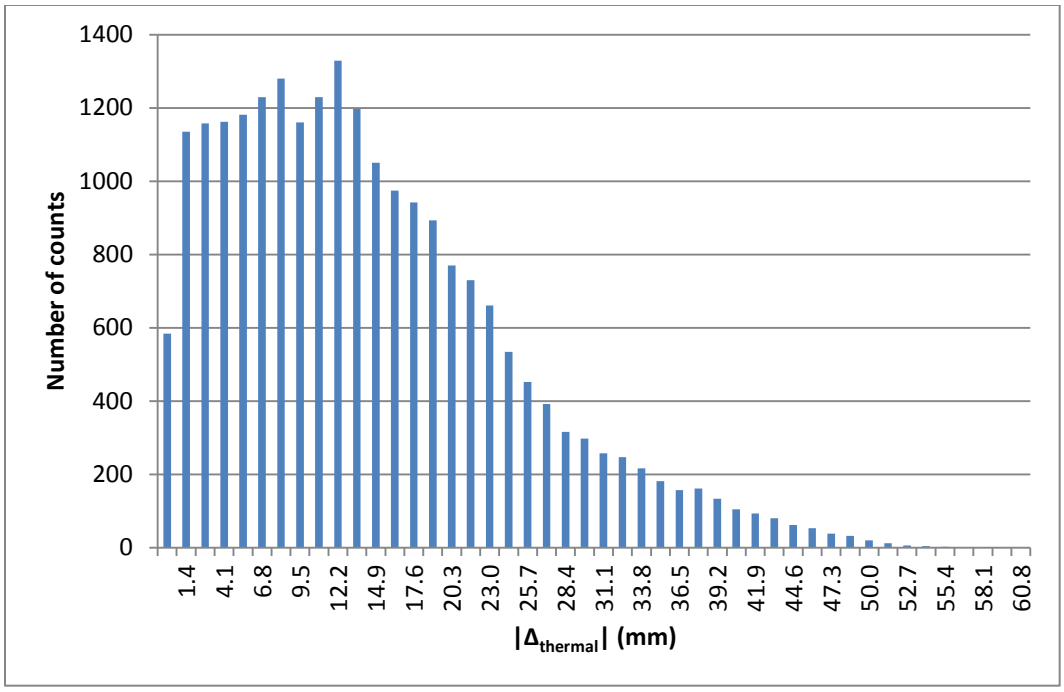

Figure 4.21: Histogram of $|\Delta_{thermal}|$ for the A30 Bridge from 1980-2010 (Montreal climate)

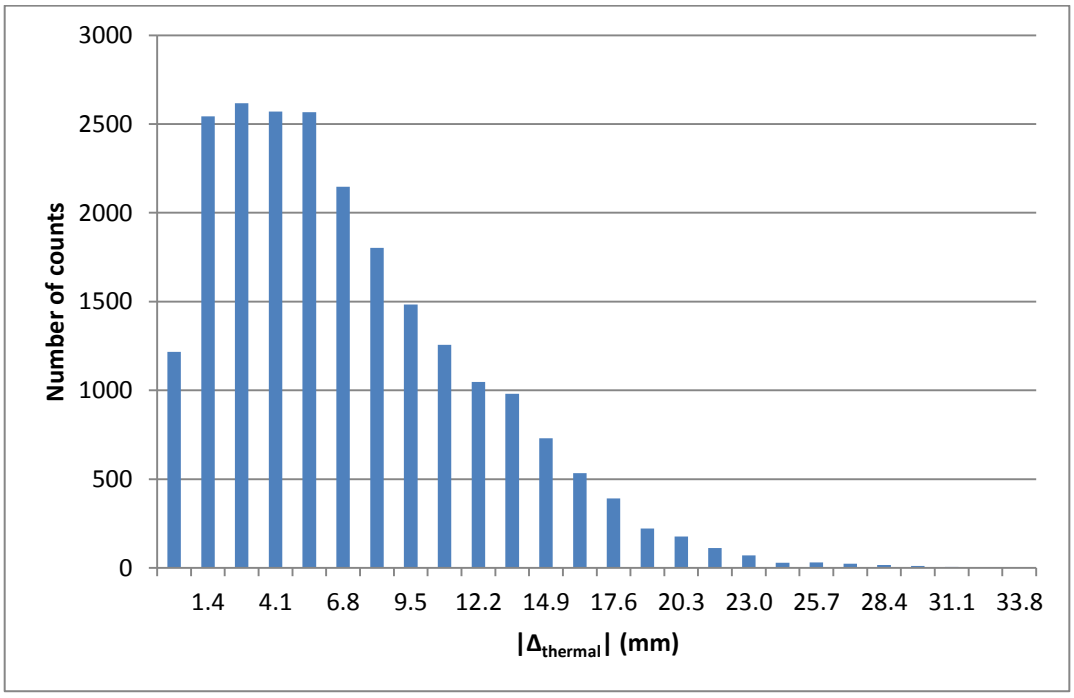

Figure 4.22: Histogram of $|\Delta_{thermal}|$ for the A30 Bridge from 1980-2010 (Vancouver climate)

4.3.2 Seismic Displacements of A30 Bridge

As for the seismic displacements of the A30 Bridge isolators, equation 4.2 is utilized yet again for AB06 and AG10 hazard curves.

$$\Delta_{seismic} = S_D = (250 \times S_a \times S_i \times T^2)/B \quad (4.2)$$

where

S_a = spectral acceleration provided by the hazard curve

S_i = site coefficient which is equal to 1.0 in this thesis

T = natural period of vibration listed in Table 4.12

B = coefficient for the effective damping of the isolation system equal to 1.58

Table 4.12 and Figure 4.23 summarize the results on the following page.

Table 4.12: Seismic displacements in mm of A30 Bridge at 2%/50 years

Seismic Hazard Model	T=0.01 sec	T=0.1 sec	T=0.15 sec	T=0.2 sec	T=0.3 sec	T=0.4 sec	T=0.5 sec	T=1.0 sec	T=2.0 sec	T=3.0 sec	T=4.0 sec	T=5.0 sec	Te=2.2 sec
AB06 Montreal Site Class A	0.01	0.89	1.54	2.23	3.41	4.97	6.22	11.92	18.71	-	24.18	25.03	**19.25**
AB06 Montreal Site Class C	0.00	1.04	2.07	3.18	5.46	8.15	10.45	19.04	28.51	-	28.69	29.23	**28.53**
AG10 Montreal Site Class C	0.01	0.98	-	2.84	5.21	-	10.15	21.69	40.02	50.63	-	-	**42.14**
AG10 Montreal Site Class D	0.01	1.06	-	3.33	7.07	-	16.67	40.60	82.12	107.44	-	-	**87.18**
AG10 Vancouver Site Class C	0.01	1.90	-	7.88	14.59	-	29.63	68.43	143.86	190.29	-	-	**153.15**
AG10 Vancouver Site Class D	0.01	2.01	-	8.96	19.22	-	47.79	124.74	270.57	380.64	-	-	**292.58**

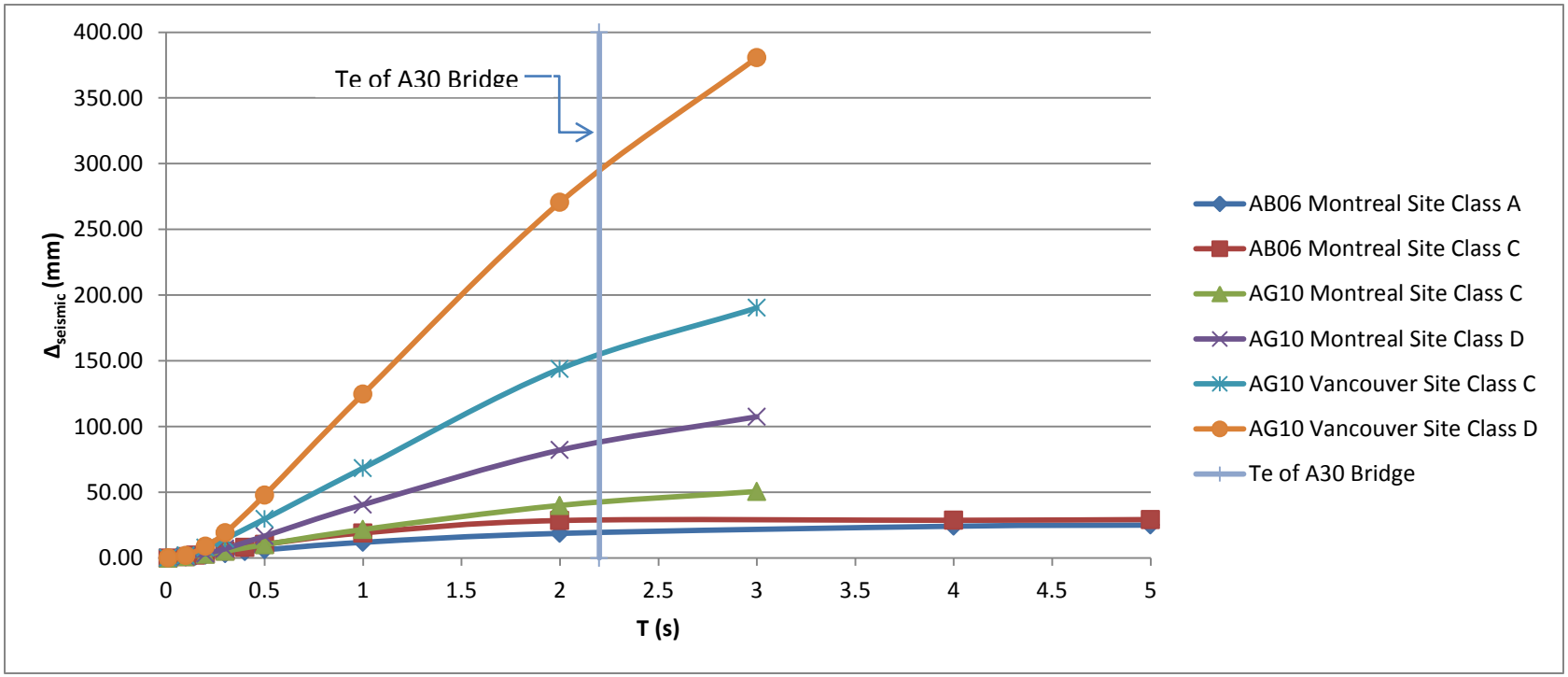

Figure 4.23: Seismic displacements of A30 Bridge according to different seismic hazard models

4.3.3 Combination of Thermal and Seismic Displacements of A30 Bridge

The amount of thermal displacement to combine with the calculated design seismic displacement for all seismic hazard models presented in this thesis are shown in Table 4.13. The total probability theorem and Turkstra's rule are again utilized. Table 4.14 incorporates the importance factor of the bridge by multiplying the seismic displacements by a factor of 1.5. Both tables are presented on the following pages.

Again, it is important to remember that both bridges are analyzed for Montreal and Vancouver's climate and seismic zoning models separately. Therefore, the A30 Bridge cannot be analyzed with Montreal's climate and Vancouver's seismic hazard model. It must be designed for both temperature and earthquake activity for a same location.

Table 4.13: $\%\Delta_{thermal}$ to combine with $\Delta_{seismic}$ for all seismic hazard models and both load combination methods for the A30 Bridge

Seismic Hazard Model	Load Combination Method	Climatic Database	T=0.5 sec	T=1.0 sec	T=2.0 sec	T=3.0 sec	T=4.0 sec	T=5.0 sec	Te=2.2 sec
AB06 Montreal Site Class A	Total Probability Theorem	Env. Canada	46.0	48.1	42.5	-	34.9	31.9	**41.8**
		CSA-S6-06	45.0	47.0	41.6	-	34.1	31.2	**40.8**
	Turkstra's Rule	Env. Canada	92.5	85.9	77.5	-	68.8	67.2	**76.6**
		CSA-S6-06	92.7	86.2	78.0	-	69.5	68.0	**77.1**
AB06 Montreal Site Class C	Total Probability Theorem	Env. Canada	42.1	47.4	39.2	-	35.9	33.7	**38.9**
		CSA-S6-06	41.2	46.4	38.4	-	35.2	32.9	**38.1**
	Turkstra's Rule	Env. Canada	87.5	77.3	65.6	-	63.8	62.7	**65.4**
		CSA-S6-06	87.7	77.8	66.3	-	64.6	63.5	**66.2**
AG10 Montreal Site Class C	Total Probability Theorem	Env. Canada	28.4	35.1	31.8	30.5	-	-	**31.6**
		CSA-S6-06	27.8	34.4	31.2	29.8	-	-	**30.9**
	Turkstra's Rule	Env. Canada	86.7	71.1	45.9	31.0	-	-	**42.9**
		CSA-S6-06	87.0	71.8	47.0	32.5	-	-	**44.1**
AG10 Montreal Site Class D	Total Probability Theorem	Env. Canada	31.7	32.6	28.2	27.2	-	-	**28.0**
		CSA-S6-06	31.0	31.9	27.5	26.6	-	-	**27.4**
	Turkstra's Rule	Env. Canada	79.8	49.0	23.7	23.7	-	-	**23.7**
		CSA-S6-06	80.2	50.1	23.2	23.2	-	-	**23.2**
AG10 Vancouver Site Class C	Total Probability Theorem	Env. Canada	26.8	23.9	23.9	23.7	-	-	**23.9**
		CSA-S6-06	28.0	24.9	24.9	24.7	-	-	**24.9**
	Turkstra's Rule	Env. Canada	40.2	20.4	20.4	20.4	-	-	**20.4**
		CSA-S6-06	37.7	21.2	21.2	21.2	-	-	**21.2**
AG10 Vancouver Site Class D	Total Probability Theorem	Env. Canada	25.0	23.5	23.4	22.9	-	-	**23.3**
		CSA-S6-06	26.1	24.5	24.4	23.9	-	-	**24.3**
	Turkstra's Rule	Env. Canada	20.4	20.4	20.4	20.4	-	-	**20.4**
		CSA-S6-06	0.2	21.2	21.2	21.2	-	-	**21.2**

Table 4.14: $\%\Delta_{thermal}$ to combine with $\Delta_{seismic}$ when importance factor is taken into consideration for the A30 Bridge

Seismic Hazard Model	Load Combination Method	Climatic Database	T=0.5 sec	T=1.0 sec	T=2.0 sec	T=3.0 sec	T=4.0 sec	T=5.0 sec	Te=2.2 sec
I = 1.5 AB06 Montreal Site Class A	Total Probability Theorem	Env. Canada	45.8	51.3	40.3	-	33.5	32.7	**39.6**
		CSA-S6-06	44.8	50.2	39.4	-	32.8	32.0	**38.7**
	Turkstra's Rule	Env. Canada	88.8	78.8	66.2	-	53.2	50.9	**64.9**
		CSA-S6-06	89.0	79.2	67.0	-	54.2	51.9	**65.7**
I = 1.5 AB06 Montreal Site Class C	Total Probability Theorem	Env. Canada	48.8	39.8	32.2	-	32.0	31.1	**32.2**
		CSA-S6-06	47.8	38.9	31.5	-	31.3	30.4	**31.5**
	Turkstra's Rule	Env. Canada	81.2	66.0	48.4	-	45.8	44.1	**48.1**
		CSA-S6-06	81.6	66.7	49.5	-	46.9	45.3	**49.2**
I = 1.5 AG10 Montreal Site Class C	Total Probability Theorem	Env. Canada	34.0	34.7	29.0	27.5	-	-	**28.7**
		CSA-S6-06	33.3	34.0	28.4	26.9	-	-	**28.1**
	Turkstra's Rule	Env. Canada	80.0	56.7	23.7	23.7	-	-	**23.7**
		CSA-S6-06	80.5	57.6	23.2	23.2	-	-	**23.2**
I = 1.5 AG10 Montreal Site Class D	Total Probability Theorem	Env. Canada	37.9	28.4	27.5	26.6	-	-	**27.3**
		CSA-S6-06	37.1	27.7	26.9	26.0	-	-	**26.7**
	Turkstra's Rule	Env. Canada	69.6	23.7	23.7	23.7	-	-	**23.7**
		CSA-S6-06	70.3	25.2	23.2	23.2	-	-	**23.2**
I = 1.5 AG10 Vancouver Site Class C	Total Probability Theorem	Env. Canada	23.4	21.0	20.8	20.9	-	-	**20.8**
		CSA-S6-06	24.4	21.9	21.7	21.7	-	-	**21.7**
	Turkstra's Rule	Env. Canada	20.4	20.4	20.4	20.4	-	-	**20.4**
		CSA-S6-06	21.2	21.2	21.2	21.2	-	-	**21.2**
I = 1.5 AG10 Vancouver Site Class D	Total Probability Theorem	Env. Canada	24.3	22.5	20.8	20.8	-	-	**20.8**
		CSA-S6-06	25.3	23.4	21.7	21.7	-	-	**21.7**
	Turkstra's Rule	Env. Canada	20.4	20.4	20.4	20.4	-	-	**20.4**
		CSA-S6-06	0.2	21.2	21.2	21.2	-	-	**21.2**

To calculate the effects of temperature on the performance of the isolators, Tables 4.10 and 4.11 developed by HITEC are again used (HITEC, 1998a & 1998b). The new periods of isolated structure Te and equivalent viscous dampings β are calculated hereunder for LRBS:

According to the 1998 HITEC report, at -28.9 ^{0}C (-20 ^{0}F), K increases by 56 %.

Therefore by using equation 1.2,

$$T = 2\pi\sqrt{\frac{M}{K}} \tag{1.2}$$

$$T \text{ @ } -28.9\ ^0\text{C} = 1.76 < 2.2 \text{ sec}$$

Also, at -28.9 ^{0}C (-20 ^{0}F), β decreases by 3 %.

$$\beta \text{ @ } -28.9\ ^0\text{C} = 24.0\ \% \text{ x } 0.97 = 23.28\ \%$$

Thus, from Table 4.8 of the CHBDC CSA-S6-06, B @ 23.28 % = 1.57

However, at 48.9 ^{0}C (120 ^{0}F), K decreases by 5 %. So, by using equation 1.2 again,

$$T \text{ @ } 48.9\ ^0\text{C} = 2.26 > 2.2 \text{ sec}$$

And, at 48.9 ^{0}C (120 ^{0}F), β decreases by 7 %.

$$\beta \text{ @ } 48.9\ ^0\text{C} = 24.0\ \% \text{ x } 0.93 = 22.32\ \%$$

Hence, from Table 4.8 of CHBDC CSA-S6-06, B @ 22.32 % = 1.55

As for FPI bearings:

At -40 ^{0}C (-40 ^{0}F), K does not change.

$$T \text{ @ } -40\ ^0\text{C} = 2.2 = 2.2 \text{ sec}$$

And, At -40 ^{0}C (-40 ^{0}F), β decreases by 6 %.

$$\beta \text{ @ } -40\ ^0\text{C} = 24.0\ \% \text{ x } 0.94 = 22.56\ \%$$

Thus, from Table 4.8 of the CHBDC CSA-S6-06, B @ 22.56 % = 1.55

However, at 48.9 ^{0}C (120 ^{0}F), K decreases by 9 %. Consequently, with equations 1.3 and 1.4 below,

$$K = \frac{W}{R} \tag{1.3}$$

$$T = 2\pi\sqrt{\frac{R}{g}} \tag{1.4}$$

T @ 48.9 ^{0}C = 2.31 > 2.2 sec

And, at 48.9 ^{0}C (120 ^{0}F), β decreases by 10 %.

β @ 48.9 ^{0}C = 24.0 % x 0.90 = 21.6 %

Therefore, from Table 4.8 of the CHBDC CSA-S6-06, B @ 21.6 % = 1.532

The values of K and B are illustrated graphically in Figures 4.24 and 4.25.

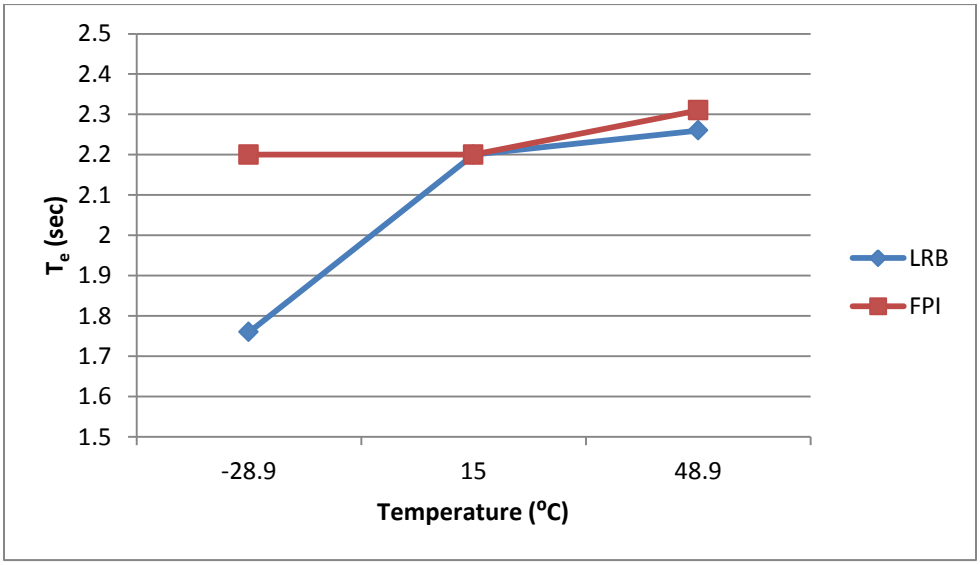

Figure 4.24: T_e values for Madrid Bridge

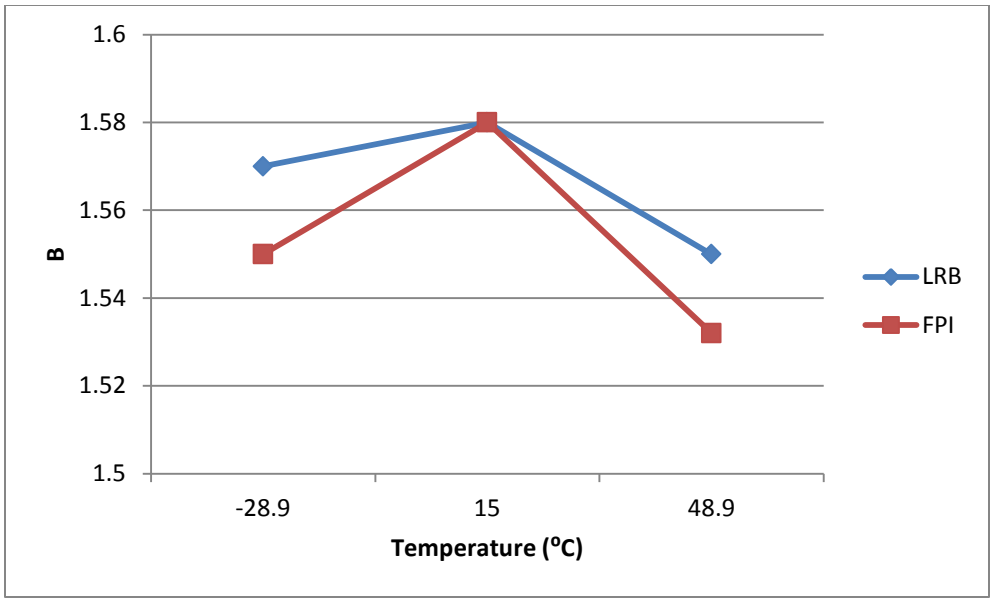

Figure 4.25: B values for Madrid Bridge

Table 4.15 on the following page summarizes the results when the performance characteristics of the bearings are taken into consideration for the A30 Bridge over the St-Lawrence River. Also, the importance factor is once more incorporated into the design by multiplying the design seismic displacements by a factor of 1.5.

Table 4.15: $\%\Delta_{thermal}$ to combine with $\Delta_{seismic}$ when performance characteristics and importance factor of bridge are taken into consideration for the A30 Bridge

Seismic Hazard Model	Bearing Type	Climatic Data	T=0.5 sec	T=1.0 sec	T=2.0 sec	T=3.0 sec	T=4.0 sec	T=5.0 sec	Te=2.2 sec
AB06 Montreal Site Class A	LRB	Env. Canada	37.5	48.1	42.5	-	35.0	32.9	**41.8**
		CSA-S6-06	36.7	47.0	41.6	-	34.2	32.2	**40.9**
	FPI	Env. Canada	37.5	48.1	42.6	-	35.1	33.0	**41.8**
		CSA-S6-06	36.7	47.0	41.7	-	34.3	32.3	**40.9**
I=1.5 AB06 Montreal Site Class A	LRB	Env. Canada	45.8	49.4	40.3	-	33.7	32.9	**39.7**
		CSA-S6-06	44.8	48.3	39.4	-	32.9	32.2	**38.8**
	FPI	Env. Canada	45.8	49.4	40.4	-	33.8	33.1	**39.7**
		CSA-S6-06	44.8	48.3	39.5	-	33.1	32.3	**38.9**
AB06 Montreal Site Class C	LRB	Env. Canada	42.1	47.4	38.6	-	36.6	35.1	**38.4**
		CSA-S6-06	41.2	46.4	37.7	-	35.8	34.3	**37.5**
	FPI	Env. Canada	42.2	47.4	38.7	-	36.8	35.2	**38.5**
		CSA-S6-06	41.2	46.4	37.8	-	36.0	34.4	**37.6**
I=1.5 AB06 Montreal Site Class C	LRB	Env. Canada	50.8	39.9	32.4	-	32.7	31.7	**32.4**
		CSA-S6-06	49.7	39.0	31.7	-	32.0	31.0	**31.7**
	FPI	Env. Canada	50.8	39.9	32.5	-	32.9	31.9	**32.6**
		CSA-S6-06	49.7	39.1	31.8	-	32.2	31.2	**31.9**
AG10 Montreal Site Class C	LRB	Env. Canada	28.5	35.2	32.0	30.7	-	-	**31.8**
		CSA-S6-06	27.8	34.4	31.3	30.1	-	-	**31.1**
	FPI	Env. Canada	28.5	35.3	32.2	30.9	-	-	**32.0**
		CSA-S6-06	27.9	34.5	31.5	30.3	-	-	**31.3**
I=1.5 AG10 Montreal Site Class C	LRB	Env. Canada	34.1	34.8	29.4	27.9	-	-	**29.1**
		CSA-S6-06	33.3	34.1	28.7	27.3	-	-	**28.5**
	FPI	Env. Canada	34.1	35.0	29.7	28.3	-	-	**29.4**
		CSA-S6-06	33.4	34.2	29.0	27.7	-	-	**28.8**
AG10 Montreal Site Class D	LRB	Env. Canada	31.7	32.8	28.6	27.8	-	-	**28.4**
		CSA-S6-06	31.0	32.1	28.0	27.2	-	-	**27.8**
	FPI	Env. Canada	31.8	33.0	29.0	28.3	-	-	**28.8**
		CSA-S6-06	31.1	32.3	28.3	27.6	-	-	**28.2**
I=1.5 AG10 Montreal Site Class D	LRB	Env. Canada	39.1	28.7	28.2	27.5	-	-	**28.0**
		CSA-S6-06	38.3	28.1	27.5	26.9	-	-	**27.4**
	FPI	Env. Canada	39.2	29.0	28.7	28.2	-	-	**28.6**
		CSA-S6-06	38.4	28.3	28.1	27.6	-	-	**28.0**
AG10 Vancouver Site Class C	LRB	Env. Canada	26.9	24.0	24.5	24.5	-	-	**24.5**
		CSA-S6-06	28.0	25.0	25.5	25.5	-	-	**25.5**
	FPI	Env. Canada	27.0	24.3	25.2	25.4	-	-	**25.2**
		CSA-S6-06	28.1	25.3	26.2	26.4	-	-	**26.3**
I=1.5 AG10 Vancouver Site Class C	LRB	Env. Canada	23.5	21.2	21.6	22.0	-	-	**21.7**
		CSA-S6-06	24.5	22.1	22.5	22.9	-	-	**22.6**
	FPI	Env. Canada	23.7	21.6	22.4	23.1	-	-	**22.6**
		CSA-S6-06	24.7	22.5	23.4	24.0	-	-	**23.5**
AG10 Vancouver Site Class D	LRB	Env. Canada	25.1	24.0	24.7	25.1	-	-	**24.8**
		CSA-S6-06	26.1	25.0	25.7	26.1	-	-	**25.8**
	FPI	Env. Canada	25.3	24.5	26.0	26.7	-	-	**26.1**
		CSA-S6-06	26.3	25.5	27.1	27.8	-	-	**27.2**
I=1.5 AG10 Vancouver Site Class D	LRB	Env. Canada	24.6	23.4	22.7	23.7	-	-	**22.9**
		CSA-S6-06	25.6	24.4	23.6	24.6	-	-	**23.8**
	FPI	Env. Canada	24.9	24.2	24.2	25.9	-	-	**24.6**
		CSA-S6-06	26.0	25.2	25.2	27.0	-	-	**25.6**

Chapter 5 Discussion

The results presented in this thesis are dependent on its input parameters, design methods and load combination formulas. The input parameters consist of climate data gathered from Environment Canada and the CHBDC CSA-S6-06 for Montreal and Vancouver, recent seismicity models developed by Gail M. Atkinson, David M. Boore and Katsuichiro Goda, and structural variables needed to determine thermal and seismic displacements. As for the design methods, the CHBDC CSA-S6-06 is utilized and the total probability theorem and Turkstra's rule are employed to combine thermal and seismic displacements. The objective of this chapter is to discuss the results produced for the Madrid Bridge and A30 Bridge in Montreal and Vancouver.

5.1 Madrid Bridge

When the performance characteristics of base isolation systems are not taken into consideration, the $\%\Delta_{thermal}$ to combine with the design $\Delta_{seismic}$ is the same for both LRB and FPI bearings. Figure 5.1 illustrates graphically the results produced for all seismicity models used in this thesis and for both load combination models.

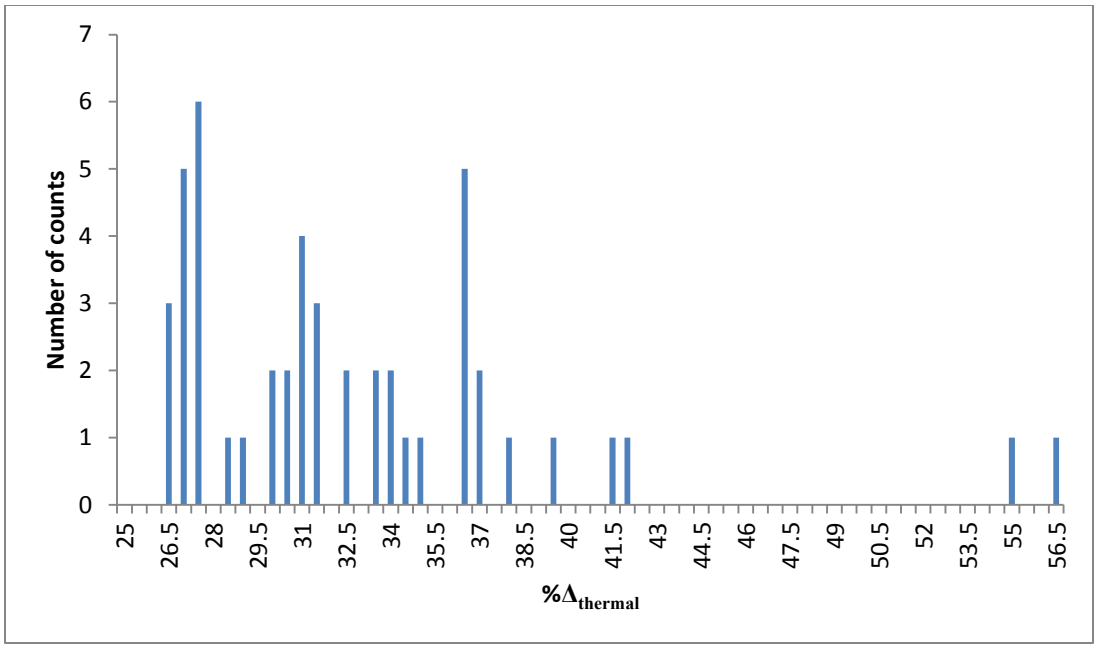

Figure 5.1: $\%\Delta_{thermal}$ to combine with the design $\Delta_{seismic}$ for the Madrid Bridge

The values of $\%\Delta_{thermal}$ from Figure 5.1 range from 26.2% to 56.5%. It is important to note that the effective temperature ranges provided by Environment Canada are fairly similar to the ones provided by the CHBDC CSA-S6-06 for Montreal. However, a significant difference exists for Vancouver. The effective temperature ranges from -10°C to 48°C with Environment Canada's data and from -9.6°C to 39.4°C with the CHBDC CSA-S6-06. Therefore, Environment Canada's ΔT and $\Delta_{thermal}$ are approximately 25% larger than those produced by the CHBDC CSA-S6 for that type of bridge in Vancouver. A more detailed portrayal of the results is shown in Table 5.1.

Table 5.1: Summary of $\%\Delta_{thermal}$ to combine with the design $\Delta_{seismic}$ for the Madrid Bridge

All Data		Montreal Data		Vancouver Data	
Range	**Frequency**	**Range**	**Frequency**	**Range**	**Frequency**
]25, 30]	18	]25, 30]	12	]25, 30]	6
]30, 35]	17	]30, 35]	15	]30, 35]	2
]35, 40]	9	]35, 40]	3	]35, 40]	6
]40, 45]	2	]40, 45]	0	]40, 45]	2
]45, 50]	0	]45, 50]	0	]45, 50]	0
]50, 55]	1	]50, 55]	1	]50, 55]	0
]55, 60]	1	]55, 60]	1	]55, 60]	0
Sum	48	Sum	32	Sum	16
Mean	32,6	Mean	32,4	Mean	32,8
Median	31,0	Median	30,8	Median	33,7
Standard Deviation	6,43	Standard Deviation	6,99	Standard Deviation	5,3
Minimum	26,2	Minimum	26,2	Minimum	27
Maximum	56,5	Maximum	56,5	Maximum	41,8
2003 Eurocode 8 Limit = 50%		**2003 Eurocode 8 Limit = 50%**		**2003 Eurocode 8 Limit = 50%**	
Pass	95,8	Pass	93,8	Pass	100
Fail	4,2	Fail	6,3	Fail	0
BC Supplement to CSA-S6-06 Limit = 40%		**BC Supplement to CSA-S6-06 Limit = 40%**		**BC Supplement to CSA-S6-06 Limit = 40%**	
Pass	91,7	Pass	93,8	Pass	87,5
Fail	8,3	Fail	6,3	Fail	12,5

Table 5.1 shows that the proportion of $\%\Delta_{thermal}$ to combine with the design $\Delta_{seismic}$ respects the 2003 Eurocode 8 limit of 50% better than British Columbia's limit of 40%. Indeed, since the Eurocode 8 limit is larger than British Columbia's limit, it will always have a failing rate lower than or equal to the Canadian Code. However, it is important to note that if the limit of $\%\Delta_{thermal}$ is set as 45% instead of 50%, the exact same success rate will occur with the results presented in Figure 5.1 and Table 5.1.

When the performance characteristics of the base isolators are taken into consideration, different results are produced. Indeed, the climate generates different load combination results for each bearing. Also, the analysis can only be performed with the total probability theorem. Figure 5.2 summarizes the results.

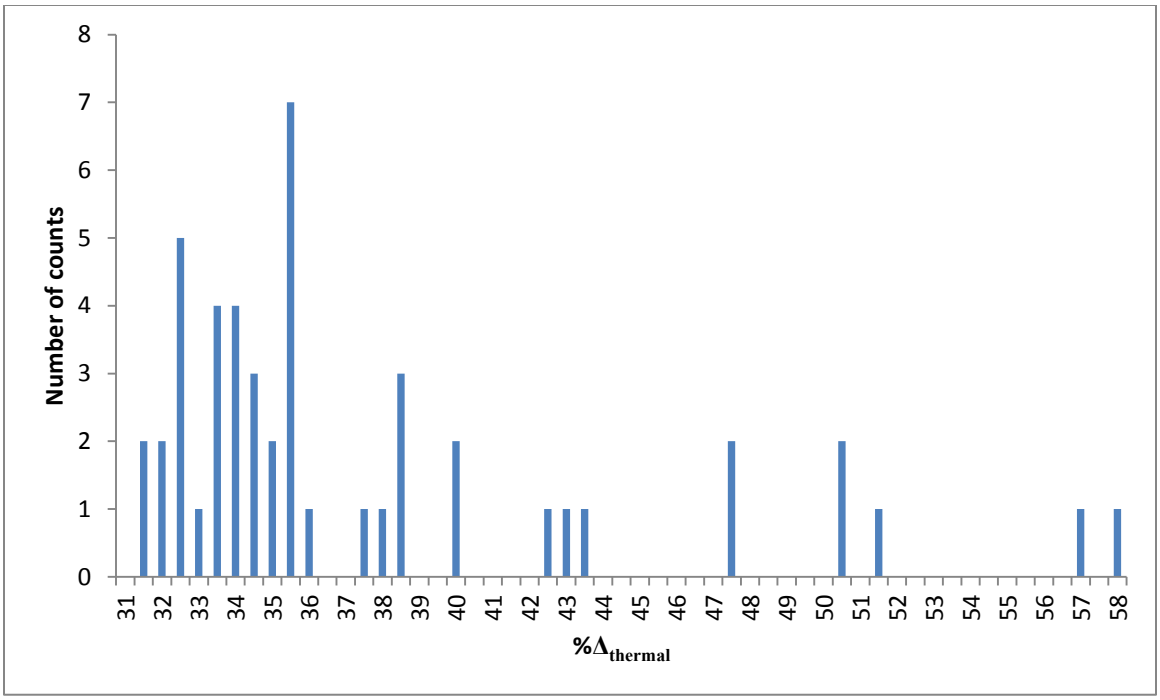

Figure 5.2: $\%\Delta_{thermal}$ to combine with the design $\Delta_{seismic}$ for the Madrid Bridge when isolator performance is considered

According to Figure 5.2, the $\%\Delta_{thermal}$ results range from 31.1% to 57.7%. The minimum value of this range is larger than the previous one, since the combined thermal and seismic displacements generated are mostly smaller than displacements for isolators unaffected by temperature. Table 5.2 summarizes results for Montreal and Vancouver exposures.

Table 5.2: Summary of $\%\Delta_{thermal}$ to combine with the design $\Delta_{seismic}$ for the Madrid Bridge when isolator performance is considered

All Data		Montreal Data		Vancouver Data	
Range	**Frequency**	**Range**	**Frequency**	**Range**	**Frequency**
]30, 35]	23	]30, 35]	22	]30, 35]	1
]35, 40]	15	]35, 40]	10	]35, 40]	5
]40, 45]	3	]40, 45]	0	]40, 45]	3
]45, 50]	2	]45, 50]	0	]45, 50]	2
]50, 55]	3	]50, 55]	0	]50, 55]	3
]55, 60]	2	]55, 60]	0	]55, 60]	2
Sum	48	Sum	32	Sum	16
Mean	37,6	Mean	34,3	Mean	44,2
Median	35,1	Median	34,0	Median	43,3
Standard Deviation	6,7	Standard Deviation	2,24	Standard Deviation	7,8
Minimum	31,1	Minimum	31,1	Minimum	32,5
Maximum	57,7	Maximum	39,9	Maximum	57,7
2003 Eurocode 8 Limit = 50%		**2003 Eurocode 8 Limit = 50%**		**2003 Eurocode 8 Limit = 50%**	
Pass	89,6	Pass	100	Pass	68,8
Fail	10,4	Fail	0	Fail	31,3
BC Supplement to CSA-S6-06 Limit = 40%		**BC Supplement to CSA-S6-06 Limit = 40%**		**BC Supplement to CSA-S6-06 Limit = 40%**	
Pass	79,2	Pass	100	Pass	37,5
Fail	20,8	Fail	0	Fail	62,5

The results of Table 5.2 are very different than the ones shown in Table 5.1. Indeed, the overall proportion of failure in the above table is much higher. Also, when the Madrid Bridge is analyzed in Montreal, British Columbia's limit of 40% is respected 100% of the time. One of the reasons why the Madrid Bridge cannot respect the 2003 Eurocode 8 limit in Vancouver more than 68.8% of the time is because it was designed to be built near Drummondville in the province of Quebec and not Montreal. According to the CSA-S6-06, Drummondville's seismic loads are quite lower than Montreal's. In fact, the CHBDC CSA-S6-06 assigns a zonal acceleration ratio equal to 0.15 g for Drummondville. This amount is 25% smaller than Montreal's ratio (CSA, 2006a).

5.2 A30 Bridge

The A30 Bridge over the St-Lawrence River has different parameters than the Madrid Bridge. Therefore, the amount of $\%\Delta_{thermal}$ to combine with the design $\Delta_{seismic}$ for base isolators is different. Figure 5.3 illustrates the range of $\%\Delta_{thermal}$ for the A30 Bridge when the performance characteristics of isolators are unaffected by the ambient temperature. Again, half of the results include the importance factor of the bridge set as 1.5.

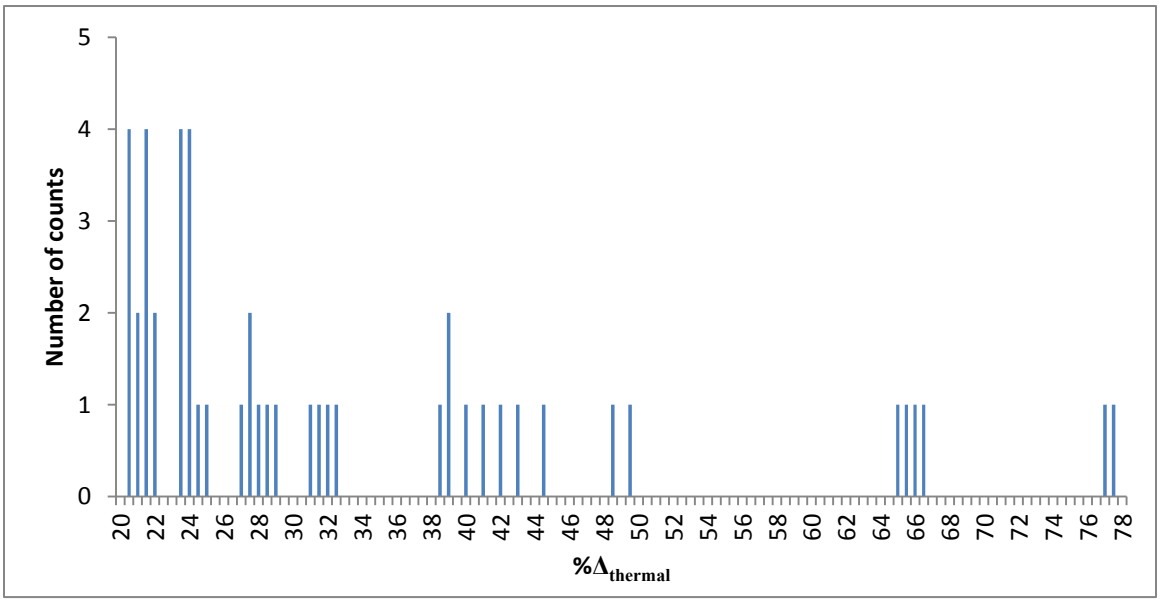

Figure 5.3: $\%\Delta_{thermal}$ to combine with the design $\Delta_{seismic}$ for the A30 Bridge

The values of $\%\Delta_{thermal}$ represented in Figure 5.3 can be as low as 20.4%, and as high as 77.1%. Turkstra's rule is mainly responsible for these high proportions. Table 5.3 presents a more detailed portrait of the amount of $\%\Delta_{thermal}$ to combine with the design $\Delta_{seismic}$ for the A30 Bridge, and helps quantify the unreliable results produced by Turkstra's rule.

Table 5.3: Summary of $\%\Delta_{thermal}$ to combine with the design $\Delta_{seismic}$ for the A30 Bridge

All Data		Montreal Data		Vancouver Data	
Range	**Frequency**	**Range**	**Frequency**	**Range**	**Frequency**
]20, 25]	22	]20, 25]	6	]20, 25]	16
]25, 30]	6	]25, 30]	6	]25, 30]	0
]30, 35]	4	]30, 35]	4	]30, 35]	0
]35, 40]	4	]35, 40]	4	]35, 40]	0
]40, 45]	4	]40, 45]	4	]40, 45]	0
]45, 50]	2	]45, 50]	2	]45, 50]	0
]50, 55]	0	]50, 55]	0	]50, 55]	0
]55, 60]	0	]55, 60]	0	]55, 60]	0
]60, 65]	1	]60, 65]	1	]60, 65]	0
]65, 70]	3	]65, 70]	3	]65, 70]	0
]70, 75]	0	]70, 75]	0	]70, 75]	0
]75, 80]	2	]75, 80]	2	]75, 80]	0
Sum	48	Sum	32	Sum	16
Mean	33,7	Mean	39,7	Mean	21,7
Median	27,4	Median	35,2	Median	21,2
Standard Deviation	15,86989601	Standard Deviation	16,41415597	Standard Deviation	1,500166657
Minimum	20,4	Minimum	23,2	Minimum	20,4
Maximum	77,1	Maximum	77,1	Maximum	24,9
2003 Eurocode 8 Limit = 50%		**2003 Eurocode 8 Limit = 50%**		**2003 Eurocode 8 Limit = 50%**	
Pass	87,5	Pass	81,3	Pass	100
Fail	12,5	Fail	18,8	Fail	0
BC Supplement to CSA-S6-06 Limit = 40%		**BC Supplement to CSA-S6-06 Limit = 40%**		**BC Supplement to CSA-S6-06 Limit = 40%**	
Pass	75,0	Pass	62,5	Pass	100
Fail	25,0	Fail	37,5	Fail	0

From Table 5.3, only 6 results out of 48 are higher than the 2003 Eurocode 8 limit of 50%. In other words, 12.5% of the data is exaggerated and should be discarded. Therefore, setting the design limit at 50% for bridge base isolators is still considered a reliable and efficient bridge standard. Also, it is important to realize from the above table that if the A30 Bridge was built in Vancouver, it would easily satisfy British Columbia's limit of 40%. As a matter of fact, 24.9% is the highest %Δthermal generated from both load combination methods in that city.

When the performance characteristics of the base isolators are considered in the analysis, different results are yet again produced. Figure 5.4 demonstrates the results.

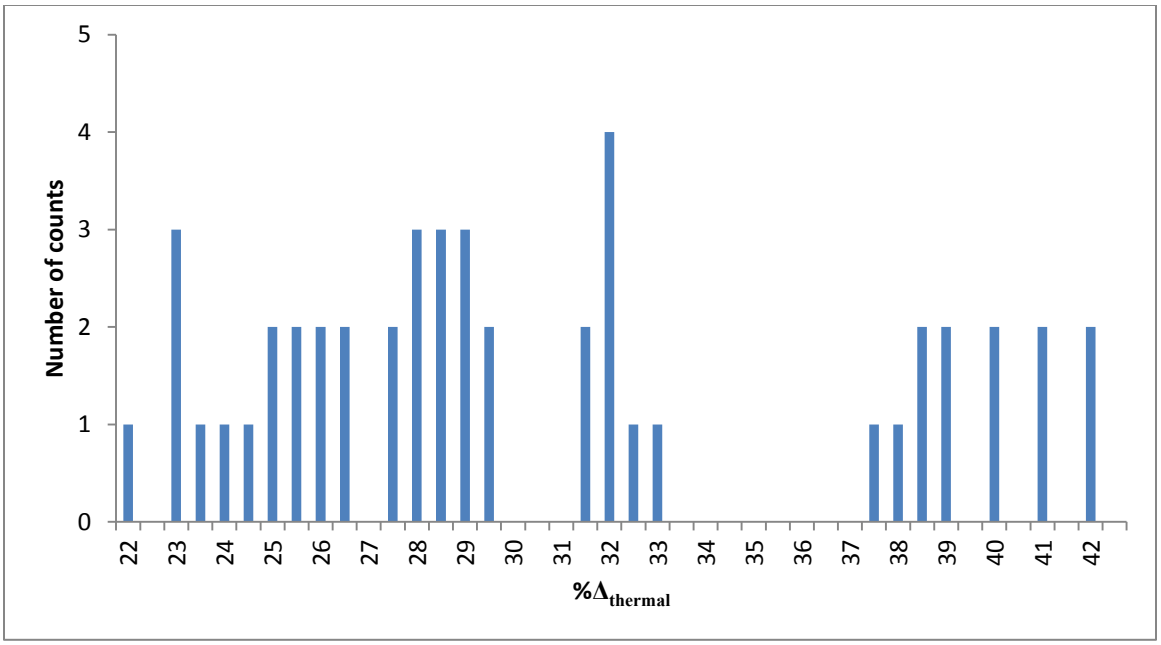

Figure 5.4: $\%\Delta_{thermal}$ to combine with the design $\Delta_{seismic}$ for the A30 Bridge when isolator performance is considered

The values of $\%\Delta_{thermal}$ range from 21.7% to 41.8%. This range is much more consistent than the previous ranges, and satisfies the 2003 Eurocode 8 limit of 50%. Also, it is important to know that even the $\%\Delta_{thermal}$ values produced by Turkstra's rule respect the 50% limit. Again, Table 5.4 on the next page provides a statistical resume of the results.

Table 5.4: Summary of $\%\Delta_{thermal}$ to combine with the design $\Delta_{seismic}$ for the A30 Bridge when isolator performance is considered

All Data		Montreal Data		Vancouver Data	
Range	**Frequency**	**Range**	**Frequency**	**Range**	**Frequency**
]20, 25]	9	]20, 25]	0	]20, 25]	9
]25, 30]	19	]25, 30]	12	]25, 30]	7
]30, 35]	8	]30, 35]	8	]30, 35]	0
]35, 40]	8	]35, 40]	8	]35, 40]	0
]40, 45]	4	]40, 45]	4	]40, 45]	0
]45, 50]	0	]45, 50]	0	]45, 50]	0
Sum	48	Sum	32	Sum	16
Mean	30,5	Mean	33,4	Mean	24,5
Median	28,7	Median	31,9	Median	24,7
Standard Deviation	6,0	Standard Deviation	5,1	Standard Deviation	1,6
Minimum	21,7	Minimum	27,4	Minimum	21,7
Maximum	41,8	Maximum	41,8	Maximum	27,2
2003 Eurocode 8 Limit = 50%		**2003 Eurocode 8 Limit = 50%**		**2003 Eurocode 8 Limit = 50%**	
Pass	100,0	Pass	100	Pass	100
Fail	0,0	Fail	0	Fail	0
BC Supplement to CSA-S6-06 Limit = 40%		**BC Supplement to CSA-S6-06 Limit = 40%**		**BC Supplement to CSA-S6-06 Limit = 40%**	
Pass	91,7	Pass	87,5	Pass	100
Fail	8,3	Fail	12,5	Fail	0

The above table reveals that the isolator units of the A30 Bridge built in Montreal may be designed for a 45% limit of the maximum thermal displacement to be combined with the design seismic displacement. And, with a failing rate as low as 8.3% for all the available data, one may even design the base isolators with a limit of 40% and still achieve a relatively reliable design.

Finally, since Turkstra's rule cannot take into consideration time-varying performance characteristics of base isolation systems due to climate change, and often produces unreliable results, the amount of thermal displacement to combine with the design seismic displacement of isolators should be established by simply using the total probability theorem. As such, Figure 5.5 summarises all the results produced by this load combination method for both bridges.

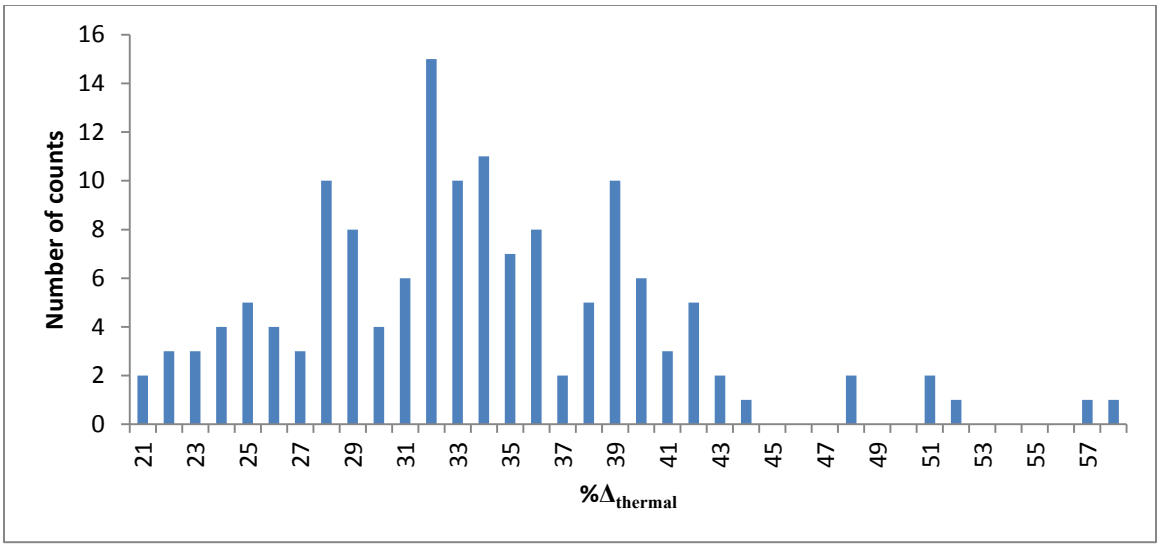

Figure 5.5: Summary of the results produced by the total probability theorem for the Madrid Bridge and A30 Bridge

As can be seen from Figure 5.5, limiting $\%\Delta_{thermal}$ to 45% is a reasonable and conservative design approach since 137 results out of all the 144 results presented in this thesis would respect this limit. This represents a solid 95% level of confidence. Furthermore, if the limit is set as 50%, only two more results would be added.

Chapter 6 Conclusion

In conclusion, this thesis shows how the total probability theorem can produce a legitimate thermal and seismic load combination formula for bridge base isolators. Thermal and seismic displacements were analyzed and combined according to basic CSA-S6-06 calculations, and the performance characteristics of the base isolation systems were also included in the design. Lastly, other load combination methods, such as Turkstra's rule, were presented in this thesis to validate its results.

It is important to note that the design of base isolators for bridges in Canada is a relatively new concept. Therefore, even though the analyses performed in this thesis revealed that 45% of the maximum thermal displacement should be combined with the design seismic displacement of bridges, engineering judgement should still be considered in the design process. Indeed, more detailed site specific analyses should be performed, since a more economical and reliable design can always be produced. Hence, the CHBDC CSA-S6 should not only recommend a displacement combination formula for the design of base isolators, such as limiting the amount of thermal displacements to 45%, but it should also allow engineers to use their judgement. This recommendation will better guide engineers, and neighbouring bridges will more likely have a consistent design which will better regulate the overall response of local bridges under future hazardous loadings.

6.1 Future Recommendations

In order to better guide bridge engineers, base isolators should be analyzed on more bridges. Indeed, bridges with different lengths, superstructure types, and capacities should be thoroughly studied. Also, all available base isolators should be analyzed with different structural parameters, such as damping coefficients, ductility and isolation periods. Once all the possible bridge parameters will be identified, they will have to be tested in all major Canadian locations. Thus, local hazards and bridges' macro and micro-climate will be considered in the design. Aggressive agents may also possibly be added to the equations in certain scenarios. This will subsequently add a level of complexity to the analysis when performance will be considered. Other performance factors may be included in the design, such as aging and maintenance. As for the calculation methods, dynamic methods and time-history analyses should be implemented to determine the design seismic displacement, instead of preliminary calculation methods. Finally, once all the possible analyses will be performed, specific limits may be established to different bridges, locations and base isolation systems for a safer, more economical and efficient design.

References

AASHTO. (2004). *AASHTO LRFD Bridge Design Specifications: U.S. Customary and SI units. (3rd ed.)*, Washington, D.C.: American Association of State Highway and Transportation Officials.

ARUP. (2011). *Montreal Autoroute 30,* http://www.arup.com/Projects/Montreal_Autoroute_30.aspx#!. (accessed 9/10/2011)

Borges, F.B.J. & Castanheta, M. (1971). *Structural Safety*, Lisboa, Portugal: Laboratorio Nacional de Engenharia Civil.

HITEC. (1998a). *Evaluation Findings for Skellerup Base Isolation Elastomeric Bearings,* http://www.asce.org/Product.aspx?ID=2147486910. (accessed 2/2/2011)

HITEC. (1998b). *Evaluation Findings for Earthquake Protection Systems, Inc. Friction Pendulum Bearings,* http://www.asce.org/Product.aspx?ID=2147486908. (accessed 2/2/2011)

Augusti, G., Baratta, A., & Casciati, F. (1984). *Probabilistic methods in structural engineering,* Chapman and Hall, New York, NY.

BC Ministry of Transportation. (2010). *Bridge Standards and Procedures Manual*, http://www.th.gov.bc.ca/publications/eng_publications/bridge/bridge_standards.htm#manual. (accessed 12/12/2010)

British Standards Institution and European Committee for Standardization. (2005). *Eurocode 8 – Design of Structures for Earthquake Resistance – Part 2: Bridges*, London: British Standards Institution.

Carleton University. (2011). *Effects of Seismicity Models and New Ground Motion Prediction Equations on Seismic Hazard Assessment for Four Canadian Cities,* http://http-server.carleton.ca/~dariush/research/Goda%20and%20Atkinson,2011.pdf. (accessed 8/1/2011)

Chen, W. F. & Duan, L. (2000). *Bridge Engineering Handbook,* Boca Raton: CRC Press.

CSA. (1966). *Design of Highway Bridges. CSA Standard S6.*

CSA. (1978). *Design of Highway Bridges. CSA Standard S6.*

CSA. (1988). *Design of Highway Bridges. CSA Standard S6.*

CSA. (2000). *Canadian Highway Bridge Design Code. CAN/CSA-S6-06 Standard.*

CSA. (2006a). *Canadian Highway Bridge Design Code*, *CAN/CSA-S6-06 Standard,* Mississauga, Ont.: Canadian Standards Association.

CSA. (2006b). *Commentary on CAN/CSA-S6-06, Canadian Highway Bridge Design Code, CAN/CSA-S6-06 Standard,* Toronto: Canadian Standards Association.

Earthquake Protection Systems. (2003). *Technical Characteristics of Friction Pendulum Bearings*, http://www.earthquakeprotection.com/TechnicalCharacteristicsofFPBearngs.pdf. (accessed 11/10/2010)

Elsevier B.V. (1983). *Combined dynamic effects of correlated load processes,* http://www.sciencedirect.com/science/article/pii/0029549383900158. (accessed 6/6/2011)

Environment Canada. (2011). *Canadian Daily Climate Data*, http://climate.weatheroffice.gc.ca/. (accessed 1/1/2011)

GeoScienceWorld. (2006). *Earthquake Ground-Motion Prediction Equations for Eastern North America*, http://bssa.geoscienceworld.org/cgi/content/full/97/3/1032. (accessed 3/1/2011)

Ghosn, M., Moses, F., & Wang, J. (2003). *Design of Highway Bridges for Extreme Events NCHRP Report 489,* Transportation Research Board, Washington, D.C.

Guizani, L. (2007). *Isolation sismique et technologies parasismiques pour les ponts au Québec: Mise au point*, 14^{e} Colloque sur la progression de la recherche québécoise sur les ouvrages d'art (In French), Québec.

Matson, D.D. & Buckland, P.G. (1995). *Experience with seismic retrofit of major bridges, Proceedings of the National Seismic Conference on Bridges and Highways: Progress in Research and Practice*, California, 10-13.

Milne, I., Ritchie, R. O., & Karihaloo, B. L. (2003). *Comprehensive Structural Integrity, Volume 2*, Elsevier Ltd. Kidlington, Oxford, UK.

Melchers, R.E. (1999). *Structural Reliability: Analysis and Prediction,* John Wiley & Sons, New York, NY.

National Research Council of Canada, Canadian Commission on Building and Fire Codes and Institute for Research in Construction. (2005). *National Building Code of Canada (NBCC)*, Ottawa: National Research Council of Canada.

Natural Resources Canada. (2011). *Fourth-generation Seismic Hazard Maps for the 2005 National Building Code of Canada*,

http://earthquakescanada.nrcan.gc.ca/hazard/13wcee/13WCEEp2502Adams_Halchuk.pdf . (accessed 3/4/2011)

NZTA. (2004). *Bridge Manual*, http://www.nzta.govt.nz/resources/bridge-manual/bridge-manual.html. (accessed 12/11/2010)

Park, R. & Blakeley, R. W.G. (1978). *Seismic Design of Bridges*, Road Research Unit, National Roads Board, Wellington, New Zealand.

Priestley, M. J. N. & Kowalsky, M. J. (2000). *Direct Displacement-based seismic Design of Concrete Buildings*, New Zealand National Society for Earthquake Engineering, Wellington, New Zealand.

Priestley, M. J. N., Seible, F., & Calvi, G. M. (1996). *Seismic design and retrofit of bridges*. New York: John Wiley & Sons.

Skinner, R. I., Robinson, W. H., & McVerry, G. H. (1993). *An introduction to seismic isolation*. Chichester: John Wiley & Sons.